

DATA MINING AND OPTIMIZATION IN STEAM-ASSISTED GRAVITY DRAINAGE
PROCESS

by

Chaoqun Li

A thesis submitted in partial fulfillment of the requirements for the degree of

Master of Science

in

Process Control

Department of Chemical and Materials Engineering

University of Alberta

©Chaoqun Li, 2018

Abstract

Steam-assisted gravity drainage (SAGD) is an enhanced oil recovery (EOR) technology widely used in Canada. Data available in SAGD industrial processes contain valuable information for monitoring, soft sensing, control, and optimization. This thesis focuses on data mining and optimization in the SAGD process, including the comparative study of machine learning algorithms, Bayesian Optimization and soft sensor design.

Subcool is a key variable of SAGD, that is important for safety and efficiency. The popular machine learning algorithms, especially those having good practical merit, are tested and compared in a subcool monitoring case. The advantages of multiple machine learning algorithms are analyzed and discussed. Moreover, investigating the original dataset suggests that data quality and priori knowledge play a vital role in applying machine learning to study data analytics problems to oil sands industry.

Bayesian Optimization considers model building and optimization simultaneously. Locally weighted quadratic regression is incorporated into the Bayesian Optimization framework, serving as the surrogate model. Details of the existing framework are tailored to use locally weighted quadratic regression as the surrogate model. Numerical cases are tested to demonstrate the usefulness of the Locally Weighted Quadratic Regression based Bayesian Optimization (LWQRBO). Additionally, the application of the proposed LWQRBO to address the formulated SAGD optimization problem is explored. Finally, optimization results show the applicability of LWQRBO in the SAGD process.

Soft sensing constructs models with data mining approaches. It is an alternative way to measure process variables when hardware sensors are not available. Stacking online soft sensor is designed for the SAGD process. The idea of stacking models inspires this design which applies multiple linear regression as a second level model,

considering ease of implementation. Two cases are studied to show the applicability and suitability of the designed soft sensor in the SAGD process.

The topics of Bayesian Optimization and ensemble models for soft sensor extend promising research directions. They are presented at the end of this thesis.

Preface

The materials presented in the thesis are part of the research project under the supervision of Professor Biao Huang and are funded by Alberta Innovates Technology Futures (AITF) and the Natural Sciences and Engineering Research Council (NSERC) of Canada.

A version of Chapter 2 of the thesis was submitted to the 10th IFAC Symposium on Advanced Control of Chemical Processes Conference. I was responsible for concept formation, program coding, data analysis, drawing conclusion as well as manuscript composition. Nabil Magbool Jan was involved in concept formation, data analysis and contributed to manuscript edits. Dr. Biao Huang was the supervisory author and was involved in manuscript composition.

Acknowledgements

First and foremost, it gives me great pleasure to acknowledge my supervisor, Dr. Biao Huang. He gave me the opportunity to explore my way in the awesome and excellent Computer Process Control (CPC) group. Dr. Biao Huang is always there to help in research. He guided me while I was trapped and lost in a research problem, encouraged me while I lost confidence, and gave me useful suggestions while I was confused about what to do next. Dr. Biao Huang is not only a professional supervisor in my research but also a life coach in how to get things done and how to live a happy life.

I appreciate Dr. Zukui Li and Dr. Csaba Szepesvári. They gave me valuable suggestions during my research. I also would like to give my thank to Nabil Magbool Jan, who had been discussing with me and helping me in the whole journey of research. I am also very grateful to Yuan Yuan, Mohammad Rashedi, Yanjun Ma, Wenhan Shen, Ruomu Tan and Seraphina Kwak. They were so helpful to me on discussing research topics, sharing ideas and figuring out solutions.

I would like give my great thank to Ming Ma and Yaojie Lu, who helped me while I was making an application to Graduate Study at University of Alberta. During my study here, I have met my exceptional CPC group members as well as those who have graduated. I next would like to thank my colleagues and friends, they are: Lei Fan, Mengqi Fang, Guoyang Yan, Gary Wang, Hashem Alighardashi, Atefeh Daemi, Zheyuan Liu, Fadi Ibrahim, Ruoxia Li, Rahul Raveendran, Shabnam Sedghi, Agustin Vicente, Anahita Sadeghian, Alireza Kheradmand, Yousef Alipouri and Kirubakaran Velswamy. I also want to thank our visiting scholars and graduated group members: Chen Xu, Ouyang Wu, Yujia Zhao, Rishik Ranjan, Yan Qin, Shunyi Zhao and Junxia Ma.

Last but not least, I owe my deepest gratitude to my parents.

Contents

1	Introduction	1
1.1	Motivation	1
1.2	Thesis Contributions	2
1.3	Thesis Outline	3
2	Data analytics for oil sands subcool prediction - a comparative study of machine learning algorithms	5
2.1	Introduction	5
2.2	Problem description	7
2.3	Revisiting selected machine learning methods	8
2.3.1	Deep Learning	8
2.3.2	Gradient Boosted Decision Trees	9
2.3.3	Random Forest	10
2.3.4	Support Vector Regression	11
2.3.5	Linear Regression and Ridge Regression	11
2.4	Model Development	11
2.4.1	Data Description	12
2.4.2	Data Pre-processing	12
2.4.3	Hyperparameter exploration	13
2.4.4	Software and Platform	16
2.5	Results and discussions	17
2.5.1	Performance on test data	17
2.5.2	Discussion	21
2.6	Data quality and priori knowledge play a vital role	22
2.6.1	Case Study on a different dataset	23

2.6.2	Investigation to original dataset and analysis	28
2.7	Conclusions	29
3	Locally Weighted Quadratic Regression based Bayesian Optimization and its application in SAGD process	30
3.1	Literature Review of Bayesian Optimization	30
3.2	Locally Weighted Quadratic Regression based Bayesian Optimization	32
3.2.1	Efficient Global Optimization	33
3.2.2	Locally Weighted Learning	35
3.2.3	Locally Weighted Quadratic Regression based Bayesian Optimization	37
3.3	Case Study	42
3.3.1	Case Study 1	43
3.3.2	Case Study 2	46
3.4	Application in simulated SAGD process	48
3.4.1	SAGD Optimization Review	49
3.4.2	Motivation and Problem Description	50
3.4.3	Optimization Results	53
3.5	Conclusions	57
4	Stacking online soft sensor application in SAGD process	58
4.1	Review of soft sensor design approaches	58
4.2	A brief introduction to the idea of stacking models	60
4.3	Revisit of Partial Least Squares Regression, Gaussian Process Regression and Support Vector Regression	61
4.3.1	Partial Least Squares Regression	62
4.3.2	Gaussian Process Regression	62
4.3.3	Support Vector Regression	63
4.4	Design of stacking online soft sensor for SAGD process	64
4.4.1	Design of the proposed soft sensor	64
4.4.2	Practicability and scalability of the designed soft sensor	67
4.5	Application of stacking online soft sensor in SAGD process	68

4.5.1	Case Study 1: Automatic Model Switching	68
4.5.2	Case Study 2: Model Performance Improvement	75
4.6	Conclusions	77
5	Conclusions	78
5.1	Summary of This Thesis	78
5.2	Directions for Future Work	79

List of Tables

2.1	Variable description for subcool prediction	12
2.2	Hyperparameter settings, Deep Learning/Deep Feedforward Neural Networks	14
2.3	Hyperparameter settings, GBDT	15
2.4	Hyperparameter settings, Random Forest	15
2.5	Hyperparameter settings, Support Vector Regression	16
2.6	Hyperparameter settings, Ridge Regression	16
2.7	Test results	17
2.8	Statistics of Deep Learning/Deep Feedforward Networks results of Section 2.5.1	21
2.9	Hyperparameter settings of new dataset, Deep Learning/Deep Feedforward Neural Networks	23
2.10	Hyperparameter settings of new dataset, GBDT	23
2.11	Hyperparameter settings of new dataset, Random Forest	24
2.12	Hyperparameter settings of new dataset, Support Vector Regression	24
2.13	Hyperparameter settings of new dataset, Ridge Regression	24
2.14	Test results of new dataset	24
3.1	Reservoir Parameters	54
3.2	Operational Bounded Constraints	54
4.1	Description of variables of simulated dataset	70
4.2	Statistical metrics on test data in Period 1	71
4.3	Statistical metrics on test data in Period 2	73
4.4	Statistical metrics on test data in Period 3	74
4.5	Statistical metrics on industrial test data	76

List of Figures

2.1	Process description	8
2.2	Architecture of Deep Feedforward Neural Networks	14
2.3	Test results of Deep Learning/Deep Feedforward Neural Networks . .	18
2.4	Test results of Gradient Boosted Decision Tree	18
2.5	Test results of Random Forest	19
2.6	Test results of Support Vector Regression	19
2.7	Test results of Ridge Regression	20
2.8	Test results of Multiple Linear Regression	20
2.9	Test results of Deep Learning/Deep Feedforward Neural Networks us- ing new dataset	25
2.10	Test results of GBDT using new dataset	26
2.11	Test results of Random Forest using new dataset	26
2.12	Test results of Support Vector Regression using new dataset	27
2.13	Test results of Ridge Regression using new dataset	27
2.14	Test results of Multiple Linear Regression using new dataset	28
2.15	Trend of Injection Tubing Pressure	29
3.1	Sampling without considering model uncertainties	33
3.2	Model uncertainties	34
3.3	Illustration of locally weighted learning	36
3.4	Flowchart of LWQRBO	42
3.5	Curve of 1-d test function	43
3.6	Performance through iterations	44
3.7	Expected Improvement of 1-d case	45
3.8	Locations of sampled points	46

3.9	Performance through iterations	47
3.10	Expected Improvement of 2-d case	48
3.11	Schematic of SAGD process	51
3.12	Optimization model elements	52
3.13	SAGD Optimization performance	55
3.14	Trend of Expected Improvement	56
3.15	Location of Initial Data and Sampled Data	57
4.1	Schematic of smart online soft sensor	65
4.2	Training and testing data partition along with timeline	69
4.3	Performance on test data in Period 1	71
4.4	Performance on test data in Period 2	72
4.5	Performance on test data in Period 3	74
4.6	Performance on industrial test data	76

Chapter 1

Introduction

1.1 Motivation

Steam-assisted gravity drainage (SAGD) is an enhanced oil recovery technology used in the extraction of bitumen from a reservoir [1]. The core process of SAGD is described as follows [1] [2]: high pressure steam is generated from a steam generator, the generated steam is then injected into the injection well and flows down to underground. Heat transfer occurs between injected steam and solid bitumen in the reservoir. Solid bitumen is heated and flows down to the production well due to gravity. A steam chamber is formed in the reservoir. Bitumen in the production well is lifted to the surface by a pump for further processing.

In the SAGD process, there exist many key variables [1] [3] such as chamber pressure, subcool, injection flowrate, injection pressure, etc. These variables are vital in processing safety and determining economic performance. Further, they play a critical role in the tasks of monitoring, control and optimization of the SAGD process. Success of these tasks relies heavily on the accuracy of the models involved in the process. Owing to complexity of the SAGD process, developing first principles based models is rather difficult. On the other hand, the oil sands industry has a large amount of data, which can be utilized to develop reliable data-driven models of the process. Therefore, in this work, data-driven models are constructed for the SAGD process.

These data-driven models can be developed for soft sensor applications to perform monitoring and for prediction. Soft sensors are alternatives to hardware sensors. In cases where hardware sensors are not available or are shut down for maintenance, soft

sensors can be used. Additionally, the data driven models constructed can be used for optimization [4] [5].

The main focus of this thesis is data mining and optimization in the SAGD process. This thesis targets data analytics and monitoring of subcool using machine learning algorithms, Bayesian Optimization to solve SAGD optimization problem, as well as soft sensor design for the SAGD process.

In each of the three main chapters, prediction models are built. In Chapter 2, subcool is predicted with multiple machine learning algorithms, all of which are global models. The regression of SOR is also performed with global models, but the performance is not satisfying. So, we build locally weighted models in Chapter 3. In Chapter 4, we still target on global models for soft sensors design, to show the design idea. More details of each main chapter are introduced in next section.

1.2 Thesis Contributions

This thesis contributes to data mining and optimization in the SAGD process. Multiple machine learning algorithms are studied for their performance in subcool monitoring. This thesis also proposes the Locally Weighted Quadratic Regression based Bayesian Optimization (LWQRBO) method. The proposed LWQRBO is then applied to optimize the SAGD process. A stacking online soft sensor is designed, and its usefulness in SAGD is presented. Detailed contributions of this work are as follows:

1. A comparative study of multiple machine learning algorithms on SAGD subcool monitoring is conducted on industrial datasets. Advantages of different algorithms are discussed.
2. Investigation and analysis of the original industrial dataset of the subcool monitoring case demonstrate the factors which should be taken into, to apply machine learning tools in the oil sands industry.
3. A Locally Weighted Learning based Bayesian Optimization method is proposed, with locally weighted quadratic regression as the surrogate model in the Bayesian

Optimization framework. Two numerical test functions are presented to demonstrate the performance of the proposed LWQRBO approach.

4. An optimization problem of the SAGD process is formulated. The proposed LWQRBO approach is applied to solve this SAGD optimization problem.

5. A stacking online soft sensor is designed particularly for the SAGD process. The design details are provided. Two case studies are presented to show the effectiveness of the designed stacking online soft sensor.

1.3 Thesis Outline

The thesis is outlined as follows:

In Chapter 2, the performances of multiple machine learning algorithms in making subcool predictions with other process variables are compared. Deep Neural Networks of Deep Learning, Gradient Boosted Decision Trees, Random Forest, Support Vector Regression, Ridge Regression and Multiple Linear Regression are tested. The results are presented and the strengths of each of these algorithms are described. Also, this chapter shows the need for incorporating process knowledge in performing data analytics in the oil sands industry.

LWQRBO is proposed in Chapter 3, where locally weighted approaches in Bayesian Optimization with Expected Improvement are applied as the figure of merit. Prediction and standard error of prediction are two components of Expected Improvement (EI), and those of locally weighted quadratic regression are incorporated into EI. Two numerical test functions are investigated to elucidate the usefulness of the proposed approach. A SAGD optimization problem is formulated, and the proposed approach is applied in a simulated SAGD process to show its applicability.

In Chapter 4, a stacking online soft sensor for the SAGD process is designed. This soft sensor applies the model stacking idea. Multiple linear regression is used as the online model, to correct predictions of offline predictive models. Two case studies, Annual Reservoir Pressure soft sensor and Water Content soft sensor, demonstrate the feasibility and effectiveness of the designed stacking online soft sensor in SAGD

process.

Conclusions and directions for future work are provided in Chapter 5.

Chapter 2

Data analytics for oil sands subcool prediction - a comparative study of machine learning algorithms*

In this chapter, we do a comparative study of different machine learning algorithms on subcool monitoring of the SAGD process. This chapter focuses on developing subcool models with industrial datasets using deep learning and several other widely-used machine learning methods. In Section 2.1, a literature review of SAGD and subcool is provided. In Section 2.2, the targeted problem is formulated. Section 2.3 presents a brief description of deep learning and other selected machine learning methods. The subcool model development and corresponding hyperparameter exploration are discussed in Section 2.4. Model performances of different algorithms using industrial dataset are analyzed in Section 2.5. In Section 2.6, the vital role of data quality and priori knowledge are demonstrated. Conclusions are presented in Section 2.7.

2.1 Introduction

Steam Assisted Gravity Drainage (SAGD) is an efficient, in situ, enhanced oil recovery technique to produce heavy crude oil and bitumen from reservoirs [1]. The SAGD operation involves a well pair consisting of two wells; an injection well, and a production well. The high-temperature steam, generated from the steam genera-

*This chapter was modified to have been submitted to the 10th IFAC Symposium on Advanced Control of Chemical Processes Conference: Chaoqun Li, Nabil Magbool Jan, Biao Huang, Data analytics for oil sands subcool prediction - a comparative study of machine learning algorithms

tion system, is injected into the reservoir through the injection well which heats up and reduces the viscosity of the heavy bitumen in the reservoir, and forms the steam chamber underground. The heated bitumen and condensed liquid then flow towards the production well due to gravity. The bitumen collected in the producer is then pumped to the surface for further processing [1] [2].

In a recent review paper, the elements of SAGD success, economics and operations, mechanics and the effects of reservoir properties on SAGD have been extensively discussed [2]. In addition, the detailed review of Geo-mechanical effect and Steam-Fingering Theory on SAGD process have been discussed [3].

One of the most important variables in SAGD operations is subcool, which is the temperature difference between steam at the injector and fluid at the producer [6]. It is a key parameter which reflects the liquid level at the producer and has a significant impact on SAGD reservoir performance [6]. Yuan et al. [7] studied the relationship between subcool, wellbore drawdown, fluid productivity and liquid level. Moreover, a model for the SAGD liquid pool above the production well was studied with heat balance and mass balance equations [8].

Ito et al. [9] conducted a study on reservoir dynamics and subcool optimization for steam trap control. Subcool has been considered an important factor for Artificial Lift Systems [10]. Gotawala et al. [11] proposed a subcool control method with smart injection wells. In their study, they divided the SAGD injector into several intervals, and controlled subcool by changing the steam pressure at each interval. In addition, the study on the optimization of subcool in SAGD bitumen process has been carried out [12]. Furthermore, the Model Predictive Control technique has been used to stabilize subcool temperature and automate well operations in SAGD industry [13] [14].

Subcool not only influences reservoir and oil production performance but also has a significant effect on operational safety, since it can reflect the liquid level of the producer. An inappropriate liquid level can result in steam breakthrough thus damaging equipment. Therefore, predicting the subcool value is necessary, and it is beneficial in monitoring, control, and optimization of the process. From the monitoring point of view, the prediction model of the subcool can provide useful information to process and operations engineers. From the control or optimization point of view, the subcool

response to the operational variables is important since the subcool value plays a key role in bitumen production in addition to the steam utilization.

SAGD is a complex thermal recovery process. Since subcool is a temperature difference, and several factors which have an effect on the temperature at injector and producer will influence the subcool. For example, pump frequency will influence the liquid level trapped at the bottom of the producer, therefore, it has an effect on the temperature at the producer. Also, the heterogeneity of the reservoir properties hinders us from developing a first principle model of subcool. Researchers, therefore, often resort to developing data-driven models in this work.

2.2 Problem description

SAGD technology has been used extensively in the oil sands industry in recent decades, and a large volume of historical industrial datasets are available. With the advent of novel machine learning methods and data analytics, these historical process data can be efficiently used to improve the process performance. The stored data contains a wide variety of information such as seismic images of the steam chamber which are of image types and conventional process variables that are stored as floating point variables. Further, the enhancement in the instrumentation of the operations has increased the speed at which the data is stored. In addition, the data includes a lot of inconsistent measurement and missing values, which can be caused by the hardware sensor faults. It also has noisy measurement due to the hardware sensors and varying environment. Data in SAGD process also contains a lot of useful information that can be used efficiently to improve the process operation and increase profitability.

In this study, we aim to solve a problem of estimating an underground state variable, subcool, using some of the manipulated variables as inputs. Figure 2.1 presents the schematic of SAGD operation. The injected steam plays a significant role in subcool, and the liquids produced are lifted up by the pump. Therefore, the input variables used are those related to injector flowrate, injector pressure, and pump

frequency. In this study, we will build a prediction model of subcool as follows:

$$Y = f(X_1, X_2, \dots, X_p) \quad (2.1)$$

where Y denotes subcool at a certain location and X_1, X_2, \dots, X_p denote selected input variables. As described, we have only selected manipulated variables as influential features for the subcool prediction. The developed data-driven model is beneficial when underground hardware sensor measurement is unavailable or unreliable, and can be utilized as an alternative sensor measurement.

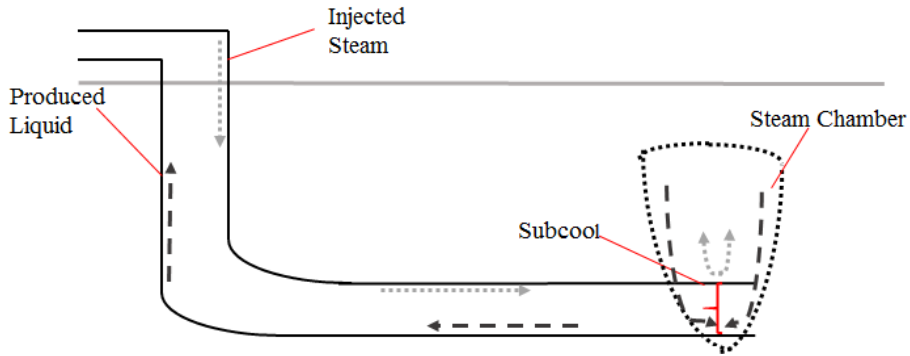


Figure 2.1: Process description

2.3 Revisiting selected machine learning methods

Machine learning includes a wide range of algorithms, such as supervised learning, unsupervised learning, reinforcement learning, transfer learning, etc. As described in Section 2.2, we will focus on solving a modelling problem for a highly complex industrial process in this work. In order to deal with complex industrial data, we resort to advanced data-driven modelling techniques. We consider several widely used algorithms including Deep Learning, ensemble tree-based methods, kernel methods and linear methods. We introduce them briefly in this section.

2.3.1 Deep Learning

Deep Learning includes a wide range of algorithms, such as Deep Neural Networks, Auto Encoders, Restricted Boltzmann Machines, Deep Belief Networks, etc. They can

perform supervised learning, semi-supervised learning and unsupervised learning [15]. There are many Deep Neural Networks types, such as Convolutional Neural Network (CNN) and Long Short Term Memory (LSTM), which have profound applications in Image Processing and Natural Language Processing, respectively [16]. Generative Adversarial Networks (GAN) is an example of the popular networks which is used in unsupervised learning algorithm [17].

In this study, we consider Deep feedforward neural networks. “Deep feedforward networks, also called feedforward neural networks, or multilayer perceptrons (MLPs), are the quintessential deep learning models” [15]. Multilayer feedforward networks have been proved to be universal approximators [18].

We next introduce some key aspects of deep feedforward network which are crucial to its performance. One of the important factors that determine the convergence of a deep network and its performance is weight initialization. There are several methods to do the initialization, via randomly sampling from a uniform or normal distribution over an interval or generating a random orthogonal matrix [19] [20] [21].

Another important factor that affects the performance of a deep learning model is the choice of the activation function. Sigmoid and hyperbolic tangent function were the popular choices of activation function in the past, and Rectified Linear Unit (ReLU) has become popular recently [16]. The mathematical form of ReLU, which is proved to improve Restricted Boltzmann Machines, can be expressed as follows [22]:

$$f(x) = \max(0, x) \tag{2.2}$$

There are some variants of ReLUs, such as Leaky ReLUs and Exponential Linear Units (ELUs) [23] [24].

Another important component in Deep Learning is the optimization algorithm. The widely used algorithms are mini-batch Stochastic gradient descent and its multiple variants [25] [26]. In this work, we will use Adam [27]. The introduction of deep learning mainly follows the works by Goodfellow et al. [15] and LeCun et al. [16].

2.3.2 Gradient Boosted Decision Trees

Gradient Boosted Decision Trees (GBDT) is one of the most widely used machine learning algorithms today. Friedman proposed gradient boosting machine [28] [29].

Gradient boosted tree method iteratively develops an additive regression model sequentially. At each iteration, it assumes that the model is imperfect and constructs a new model to be added to the existing model [30].

The basic idea of Boosting is to sequentially apply weak learners to modify the dataset in order to generate a sequence of weak predictors. As a result, the final prediction is formed by combining predictions from all weak predictors [31]. Gradient Boosting constructs weak predictors by fitting a gradient at each iteration. This gradient is that of the loss function to be minimized with respect to the model values [28] [29].

The gradient tree boosting algorithm is briefly introduced as follows [30]: It starts with building a constant regression model. To illustrate this, assume we build M trees, so there are M outer loop iterations. In each iteration, the gradient of the loss function with respect to the function values at each training data point is calculated, and a regression tree is fitted between training data points and residuals. Then, the current predictor is updated. After M iterations, the final predictor is constructed.

2.3.3 Random Forest

Random Forest was proposed by Breiman [32]. It is an ensemble of unpruned decision trees. As in Bagging, it trains each tree on a sampled bootstrap dataset from the training data. However, it considers a random subset of the variables to split an internal node, rather than all the variables. Each tree of Random Forest is a decision tree, and for a regression problem, the average value is applied as the prediction.

The training process of Random Forest can be summarized as follows [32] [33]:

1. Draw M bootstrap datasets from the training dataset. Each bootstrap dataset is sampled randomly with replacement to maintain the same size as the training data.
2. Grow a decision tree for each bootstrap dataset. A randomly selected q features are considered to split an internal node. The tree is grown until the maximum tree depth. The maximum of tree depth could be set via different ways, through tree depth, the number of samples at leaves, etc. Then M predictors are obtained.
3. Aggregate M predictions of the new data point to compute the final single prediction. The majority vote and the average value are applied for classification and regression as final prediction, respectively.

Note that some important properties of Random Forest, such as, Out-of-Bag (OOB) error, Variable Importance, and Intrinsic Proximity Measure [32] are not discussed here in the interest of brevity.

2.3.4 Support Vector Regression

Cortes and Vapnik at AT&T Labs proposed Support Vector Network as a learning machine [34]. The main idea here is to do feature expansion: First, inputs are mapped to a high dimensional space non-linearly; then, a linear surface is built in the new space. The solution of SVM is sparse, and only a subset of training data points are utilized to form the solution [35].

In order to map the inputs from the original space to a high dimensional space, a kernel function is used. Some widely used kernel functions are: linear function, polynomial function and Radial Basis function [36]. The Support Vector Regression applies an ϵ -insensitive loss function, which is proposed by Vapnik, and the optimization algorithm aims at minimizing the error bound, rather than the observed training errors [34] [35] [36]. Equation 2.3 shows its form [34]:

$$L_{\epsilon}(y, f(x)) = \begin{cases} 0 & \text{if } |y - f(x)| \leq \epsilon \\ |y - f(x)| & \text{otherwise} \end{cases}. \quad (2.3)$$

2.3.5 Linear Regression and Ridge Regression

Linear Regression is the simplest regression model. Ridge Regression is a variant of linear regression, considering shrinkage of the coefficients [30]. By adding an l_2 norm penalty to the loss function of linear regression, we obtain the loss function of Ridge Regression.

2.4 Model Development

In this section, we focus on developing data-driven models using deep learning and other machine learning methods. First, we provide the details of the dataset used in this study followed by data pre-processing steps. Next, the hyperparameter exploration and settings of the different methods are discussed. Finally, software and

platform to conduct the model developments are included.

2.4.1 Data Description

In this study, we use an industrial dataset to develop and investigate the performance of different predictive models for subcool prediction. The dataset contains 5 inputs variables, which we use as influential input variables, to predict an output variable. See Table 2.1.

Table 2.1: Variable description for subcool prediction

	Variable	Units
Output Variable	Reservoir Subcool (Referenced by engineers as an estimation of subcool)	°C
Feature 1	Injector tubing pressure	kPa
Feature 2	Injector casing pressure	kPa
Feature 3	Injector tubing flowrate	sm^3/hr
Feature 4	Injector casing flowrate	sm^3/hr
Feature 5	Pump frequency	Hz

The dataset contains 25,000 samples of measured data after data cleaning as described in Section 2.4.2. These measurements are taken over a time period of nine months. The data is divided chronologically for training and testing purposes. The first 20,000 are considered as training dataset and for tuning hyperparameters. The next 5000 samples are used for testing the out-of-sample performance of the developed predictive models. The sampling time is 10 mins and the sample value is the average value of this interval. It is assumed to achieve the steady state, thus, we build static models.

2.4.2 Data Pre-processing

The raw industrial dataset collected from the historical database might include inconsistency, missing values, and outliers. Therefore, they cannot be used directly in the model development. Hence, data pre-processing is performed prior to model development. Data cleaning involves removing inconsistent measurement, missing values, and outliers. Then, we normalize the data for scaling issues, and also, for the convergence and better performance of machine learning algorithms.

2.4.3 Hyperparameter exploration

The goal of this subsection is to explore hyperparameter settings for each of the algorithms under investigation. For this purpose, only the first 20,000 data points are used. Test data are not used in this subsection. The first 20,000 data points are divided chronologically into training and validation datasets. In this study, we evaluate the following statistics: Mean Absolute Error (MAE), Mean Square Error (MSE), Pearson correlation coefficient, and the trend of plots to compare the performance of different hyperparameter settings of each model on the validation set. We applied Grid Search, Random Search, and Greedy Search as hyperparameter search strategies. Once the hyperparameter settings are determined, we train the model again on all of the 20,000 data points to obtain the final model. This model will be used later to analyze the performance on test data. Next, we present the hyperparameter settings of different models. Description of the main hyperparameters is also discussed below. More details about hyperparameters are included in Section 2.3.

Deep Learning/Deep Feedforward Neural Networks

One of the core ideas of deep learning is to have deeper architectures [37]. Therefore, we tried multiple layers on training dataset, and finally selected 4 hidden layers. Dropout is a way to avoid overfitting [38]. Our hidden layer is not wide, and we do not apply dropout in this case. We apply l_2 norm for regularization and avoid overfitting. An epoch means a complete pass through the whole training dataset while training the model [15] [39]. The network is fully connected.

See Figure 2.2 for its architecture in this case, and Table 2.2 for its hyperparameter settings.

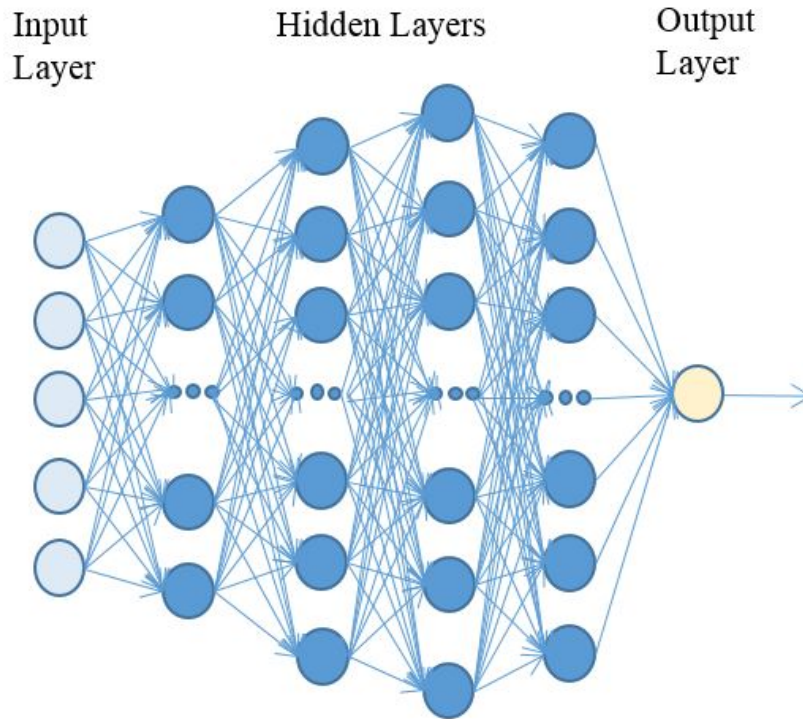


Figure 2.2: Architecture of Deep Feedforward Neural Networks

Table 2.2: Hyperparameter settings, Deep Learning/Deep Feedforward Neural Networks

Hyperparameter name and meaning	Set value or mode
Hidden Layers and the number of neurons	32, 128, 256, 128
Activation Functions of Hidden Layer	ReLU
Output Layer	1 neuron, linear function
L2 regularization parameter	1e-4
Optimizer	Adam(learning rate: 0.001)
epochs	300

Gradient Boosted Decision Trees

Learning rate shrinks the contribution of each tree when a tree is added to the model, and could be considered as a weighting factor of the additive sequentially learned models [28] [30]. Each decision tree has a maximum tree depth. The deeper a tree grows, the more complex a model becomes. Main hyperparameter settings of GBDT in this case are shown in Table 2.3.

Table 2.3: Hyperparameter settings, GBDT

Hyperparameter name and meaning	Set value or mode
The number of regression trees	250
Learning rate	0.01
Maximum regression tree depth	5

Random Forest

Minimum number of samples required to be at a leaf node controls the depth of a regression tree. While a tree is being trained, a randomly selected number of features are considered to split an internal node. The maximum number to consider equals to the square root of the total number of features in this setting. Main hyperparameter settings of Random Forest in this case are shown in Table 2.4.

Table 2.4: Hyperparameter settings, Random Forest

Hyperparameter name and meaning	Set value or mode
The number of regression trees in forest	500
Maximum features to consider in each split	The square root of the number of features
Minimum number of samples required to be at a leaf node	$0.01 \times$ the number of samples

Support Vector Regression

We choose Radial Basis Function as the kernel in this case after testing different kernel choices. Penalty parameter controls the trade-off between bias and variance. Main hyperparameter settings of SVR in this case are shown in Table 2.5.

Table 2.5: Hyperparameter settings, Support Vector Regression

Hyperparameter name and meaning	Set value or mode
Kernel function	Radial Basis Function
Penalty parameter for the error term in loss function	0.5
Kernel Parameter	10
Epsilon	0.1

Ridge Regression

Regularization parameter controls the bias and variance trade-off. Main hyperparameter settings of Ridge Regression in this case are shown in Table 2.6.

Table 2.6: Hyperparameter settings, Ridge Regression

Hyperparameter name and meaning	Set value or mode
Regularization strength parameter	2.5

Linear Regression

There is no hyperparameter in Linear Regression.

2.4.4 Software and Platform

In this work, the model developments and evaluations are performed in Python 2.7, in Mac OS X 10.11.5 environment.

First, to develop a deep learning model, we chose Keras 2.0.6 [39], which is a widely used open source neural network library in Python, and used TensorFlow 1.0.0 as its backend, which is developed by Google [40].

Second, for other machine learning methods investigated in this study, such as Random Forest, Gradient Boosted Decision Trees, Support Vector Regression, Ridge Regression and Multiple Linear Regression, we used scikit-learn version 0.18.1 [41] [42].

2.5 Results and discussions

First, we report and discuss the performance of each model on test data with the hyperparameter settings discussed in Section 2.4.3. Next, we perform analysis on the obtained results considering the characteristics of each algorithm. Only normalized data results are shown for data proprietary.

2.5.1 Performance on test data

In this subsection, we show the predictive performance of each model (see Figure 2.3 to Figure 2.8). The performance statistics of different models such as MAE, MSE, and Pearson correlation coefficient are presented in Table 2.7.

Table 2.7: Test results

Methods	Test MAE	Test MSE	Pearson Correlation Coefficient
Deep Learning	0.28615	0.16440	0.78320
GBDT	0.22425	0.10475	0.80857
Random Forest	0.23073	0.11927	0.77248
SVR	0.27219	0.17925	0.65551
Ridge Regression	0.53630	0.38927	0.26273
Linear Regression	0.53633	0.38931	0.26270

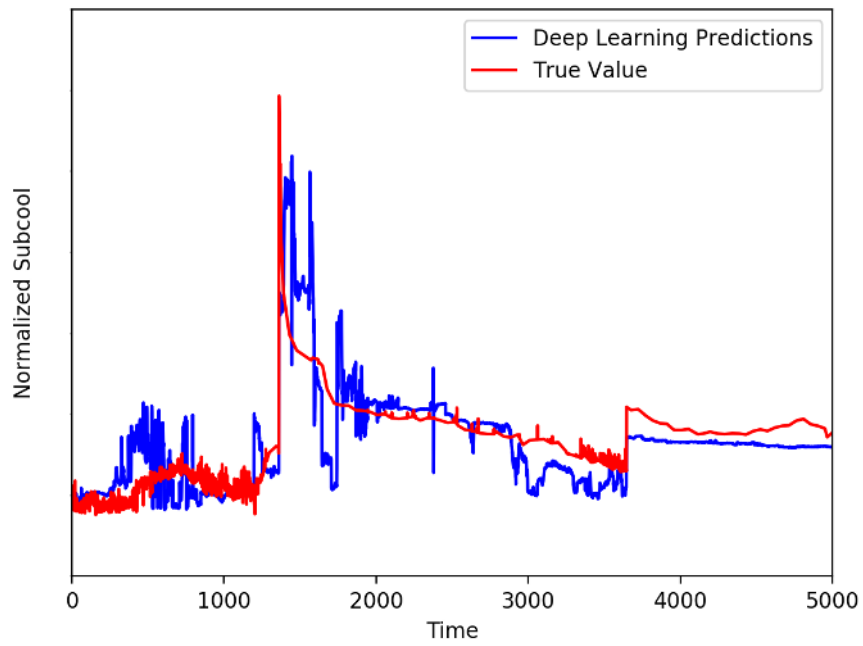


Figure 2.3: Test results of Deep Learning/Deep Feedforward Neural Networks

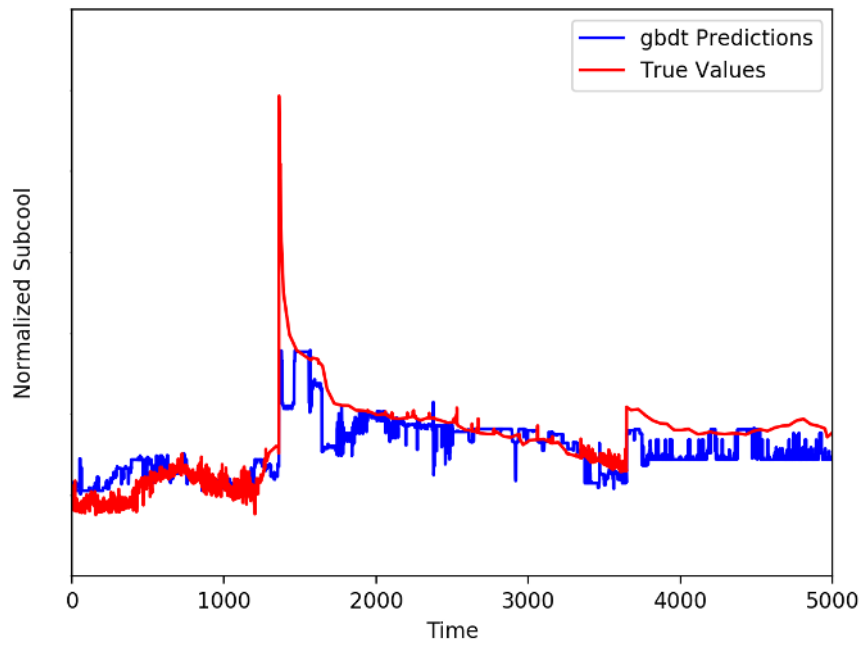


Figure 2.4: Test results of Gradient Boosted Decision Tree

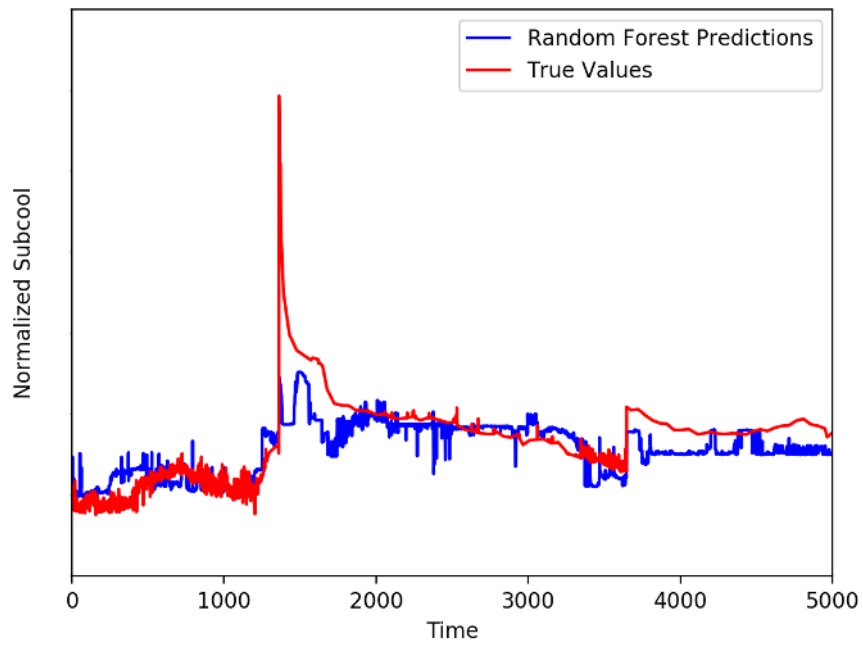


Figure 2.5: Test results of Random Forest

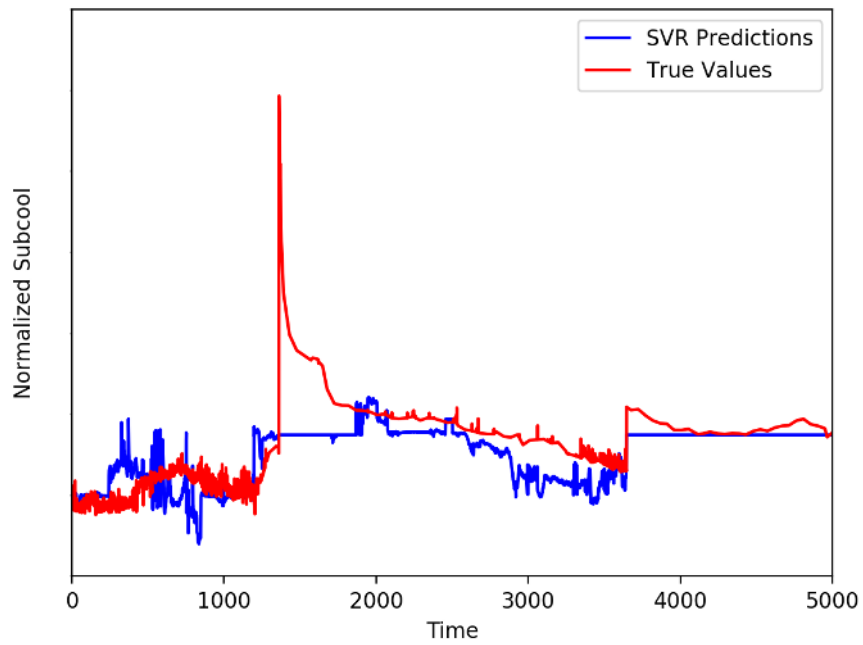


Figure 2.6: Test results of Support Vector Regression

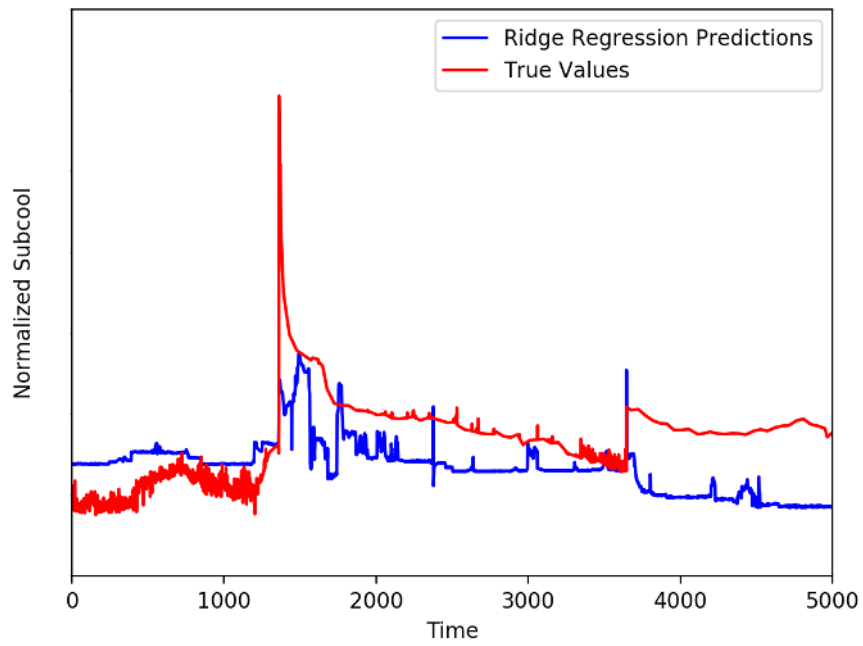


Figure 2.7: Test results of Ridge Regression

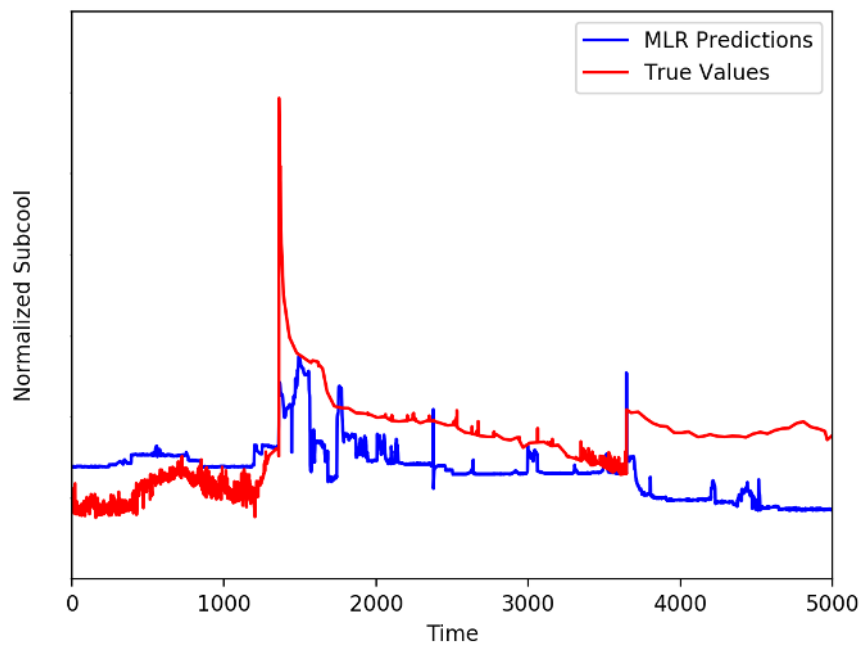


Figure 2.8: Test results of Multiple Linear Regression

While developing deep feedforward neural network model in Keras with Tensor-

Flow as its backend, we should note that the issue of randomness may lead to non-reproducible results, which comes from the random initialization weights, shuffling data, mini-batch in optimization, and implementation of tools for parallel computing [39] [40]. Strategies to solve it vary from environments, problems and motivations. In our case, to make full use of the power of mini-batch, we do not control randomness of shuffling data and mini-batch in optimization. We train the model with the same settings and data 10 times, separately. Each of the 10 models will produce a prediction. All the well-trained models are saved. Thus, we report the results with the best MAE of the 10 deep models. We apply the same strategy in Section [?]. Statistics of the 10 model results of test data are included in Table 2.8.

Table 2.8: Statistics of Deep Learning/Deep Feedforward Networks results of Section 2.5.1

Metrics Name	Minimum	Maximum	Mean	Variance
MAE	0.28615	0.44967	0.36691	0.00343
MSE	0.16339	0.35927	0.25330	0.00439
Pearson Correlation	0.70321	0.79718	0.74776	0.00112

2.5.2 Discussion

First, it is obvious that the non-linear methods have better performance compared to linear methods due to inherent nonlinearity of the dataset. Moreover, there is a slight improvement using the Ridge Regression compared to Multiple Linear Regression, since Ridge Regression shrinks coefficients. Therefore, the model is underestimated with linear methods, and a more complex model is required.

Second, it can be observed that SVR outperforms linear methods. The kernel trick in SVR doing feature expansion not only deals with data nonlinearity, but also implies that there are some hidden features in the process from the 5 input features to subcool because of its better performance than linear methods. Also, we see a relatively smoother plot in Figure 2.6. It could be explained by the threshold epsilon, which makes the prediction less sensitive to smaller noises.

Comparison between the Random Forest and GBDT indicates that GBDT performs better in terms of MAE, MSE and Pearson correlation coefficient, but both

methods perform well. As introduced earlier, both methods apply multiple models to estimate the single final prediction. Random Forest applies bagging, whereas GBDT applies boosting. This is one reason why they both perform well. Moreover, they are both based on Regression Tree. Regression Tree is trained in a quantitative way, so prediction is performed through comparison between the value of the corresponding feature and the internal nodes. As a result, both quantitative and qualitative relationships between subcool and selected features are influential in this case. In addition, using the samples of the leaf node for prediction can decrease the effect of noisy data where noise originated from environment, sensors, etc.

Deep learning method does not show the best results in terms of MAE, MSE and Pearson correlation coefficient. However, the trend plot of the Deep Learning model can capture the peak in the trend very well while all other models more or less failed in capturing the peak. This is because of the flexibility of deep learning model and powerful optimization algorithm. First, we apply multiple layers and the number of neurons in each hidden layer can be changed. Therefore, the automatic latent feature expansion and reduction within multiple hidden layers imply the meaningful results of deep feedforward neural network. Second, the ReLU activation function does not suffer from saturation problem [22]. Both of these features contribute to the flexibility of the model. Also, a good model needs a powerful optimization algorithm to train parameters. The Adam, a stochastic optimization algorithm, has the advantages of bias correction and individual adaptive learning rate, which makes it useful in solving non-convex optimization problem [27]. Hence, the model flexibility and powerful optimization algorithms make deep learning perform the best in capturing the trend.

2.6 Data quality and priori knowledge play a vital role

In this section, we show that data quality and priori knowledge play a vital role when using machine learning tools to solve oil sands problems. We first continue prediction on a new dataset following the procedure described in Section 2.4. We see that bad performance is obtained. Then, we investigate the original industrial dataset

and do more analysis on the results. The investigation and analysis emphasize the importance of data quality and priori knowledge.

2.6.1 Case Study on a different dataset

In this subsection, another set of data, containing 37,100 data points after data cleaning, is considered. The first 25,000 data points are used as training data, while the rest 12,100 data points are test data. Data normalization and model hyperparameter settings are explored again and poor performance has been reported on the new test data.

Table 2.9 to Table 2.13 show the hyperparameter settings in this dataset. As before, those hyperparameters are explored on training data.

Table 2.9: Hyperparameter settings of new dataset, Deep Learning/Deep Feedforward Neural Networks

Hyperparameter name and meaning	Set value or mode
Hidden Layers and the number of neurons	32, 128, 256, 128
Activation Functions of Hidden Layer	ReLU
Output Layer	1 neuron, linear function
L2 regularization parameter	1e-4
Optimizer	Adam(learning rate: 0.001)
epochs	300

Table 2.10: Hyperparameter settings of new dataset, GBDT

Hyperparameter name and meaning	Set value or mode
The number of regression trees	400
Learning rate	0.01
Maximum regression tree depth	5

Table 2.11: Hyperparameter settings of new dataset, Random Forest

Hyperparameter name and meaning	Set value or mode
The number of regression trees in forest	500
Maximum features to consider in each split	The square root of the number of features
Minimum number of samples required to be at a leaf node	$0.01 \times$ the number of samples

Table 2.12: Hyperparameter settings of new dataset, Support Vector Regression

Hyperparameter name and meaning	Set value or mode
Kernel function	Radial Basis Function
Penalty parameter for the error term in loss function	0.1
Kernel Parameter	5
Epsilon	0.1

Table 2.13: Hyperparameter settings of new dataset, Ridge Regression

Hyperparameter name and meaning	Set value or mode
Regularization strength parameter	2.5

The test results of statistical metrics on the new dataset are shown in Table 2.14.

Table 2.14: Test results of new dataset

Methods	Test MAE	Test MSE	Pearson Correlation Coefficient
Deep Learning	0.47431	0.31640	0.21698
GBDT	0.55289	0.44689	0.03895
Random Forest	0.53271	0.38831	0.08357
SVR	0.55324	0.40859	0.06129
Ridge Regression	0.57431	0.51714	-0.10970
Linear Regression	0.57433	0.51719	-0.10970

From Table 2.14, we learn that in this dataset, deep learning performs the best, but the performance is not as good as before. Also, all other methods perform badly.

Next, we show the trend plots of different tested methods. From Figure 2.9 to Figure 2.14, we also see that all of them failed to perform well. We will discuss why this occurs in the next subsection.

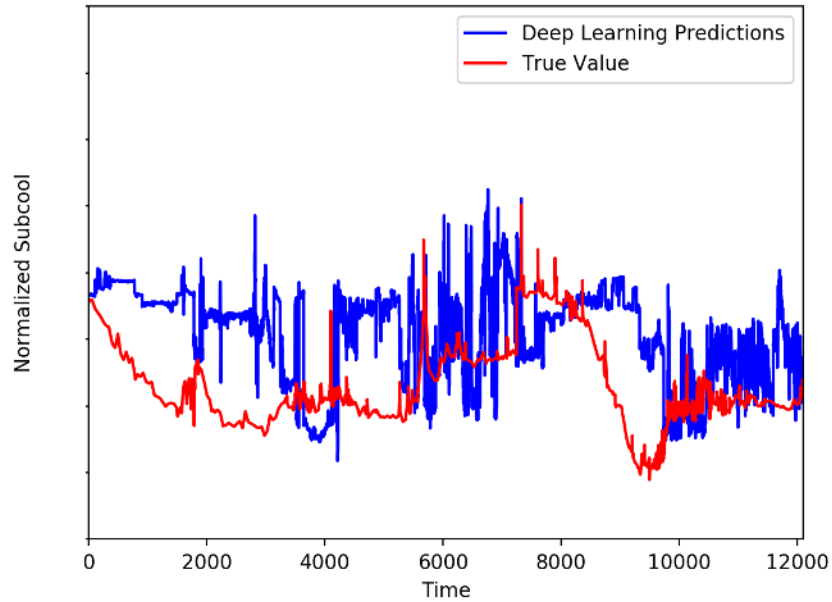


Figure 2.9: Test results of Deep Learning/Deep Feedforward Neural Networks using new dataset

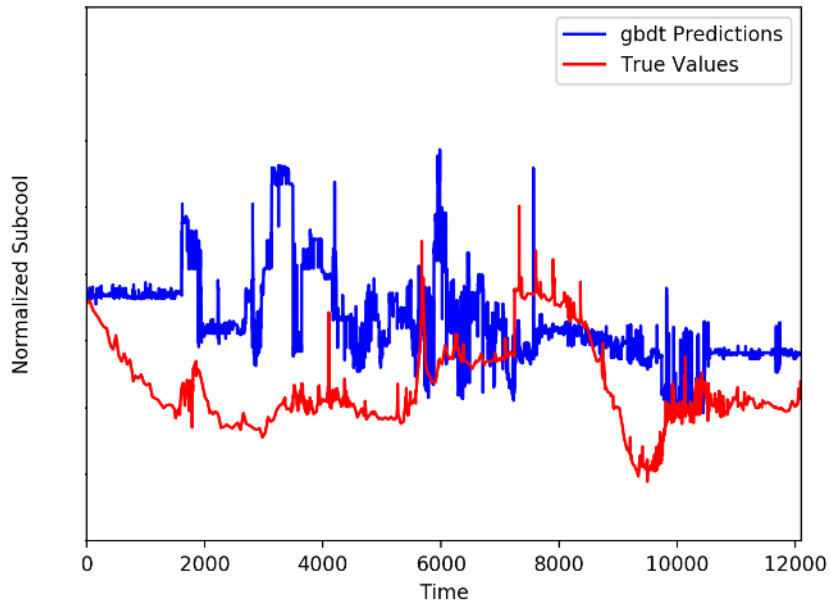


Figure 2.10: Test results of GBDT using new dataset

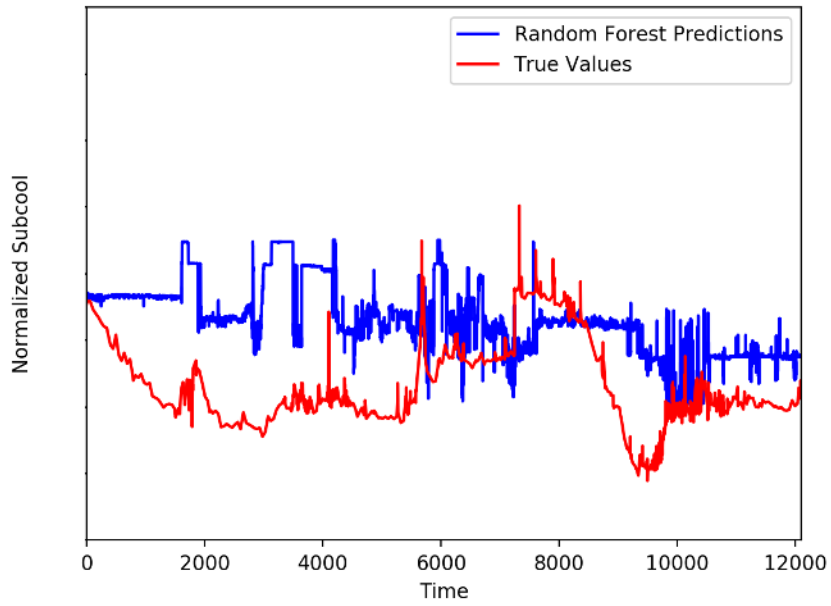


Figure 2.11: Test results of Random Forest using new dataset

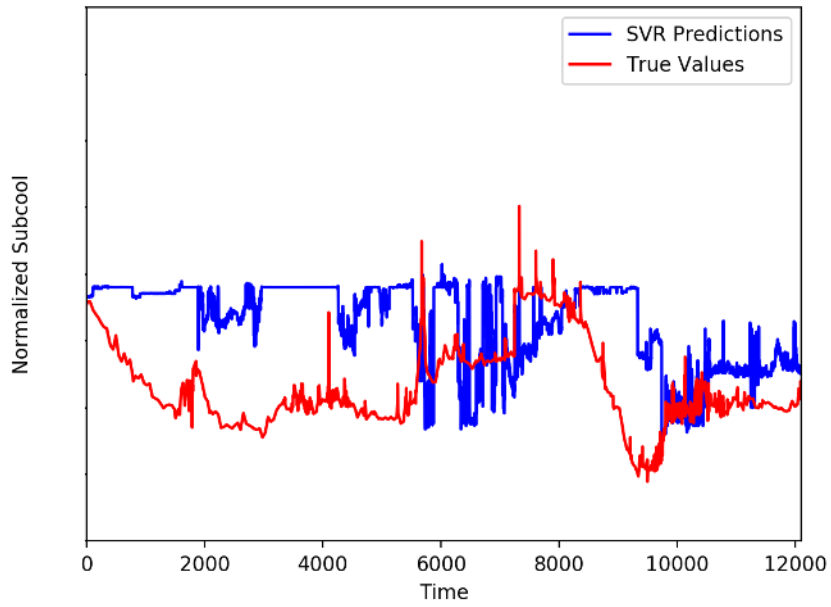


Figure 2.12: Test results of Support Vector Regression using new dataset

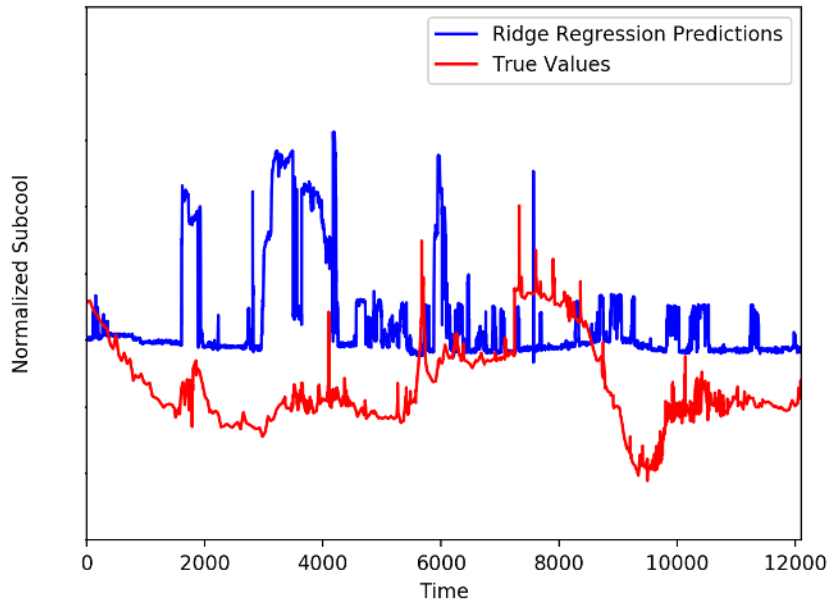


Figure 2.13: Test results of Ridge Regression using new dataset

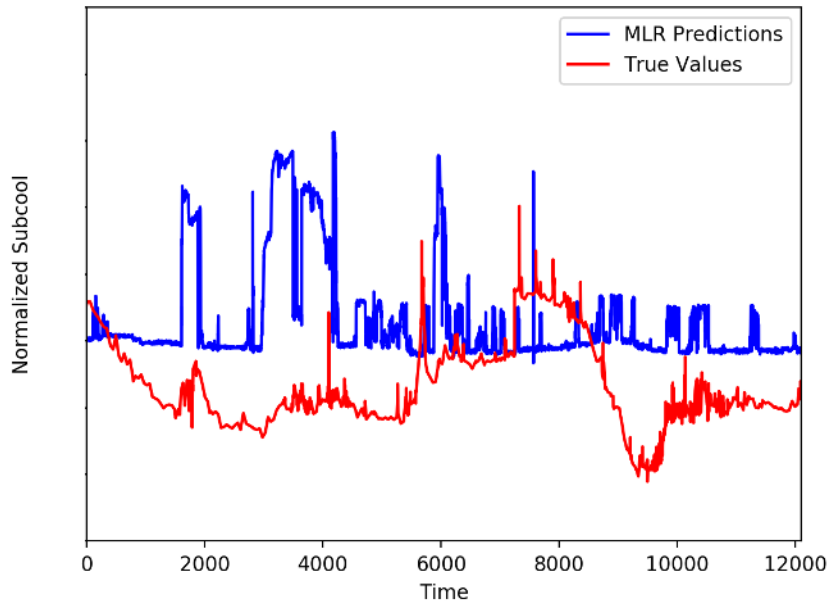


Figure 2.14: Test results of Multiple Linear Regression using new dataset

2.6.2 Investigation to original dataset and analysis

We have investigated the original data to see what occurred in the period of this set of data. We found there were obvious operation condition changes between the range of training data and testing data.

Because of closed-loop control and cascade control, the operational condition changes can be reflected by several variables. See Figure 2.15 for Injection Tubing Pressure, where training data period and testing data period is split by red dashed line. From this figure, we can see that much more significant downtrend oscillations of the injection tubing pressure occurred in the testing data period, than those occurred in the training data period, and this phenomenon has invalidated the model learned from the training data. Therefore, the data quality in engineering applications plays a critical role in the process data analytics and machine learning. Meanwhile, priori knowledge of the industrial process can also help in dealing with this type of problems.

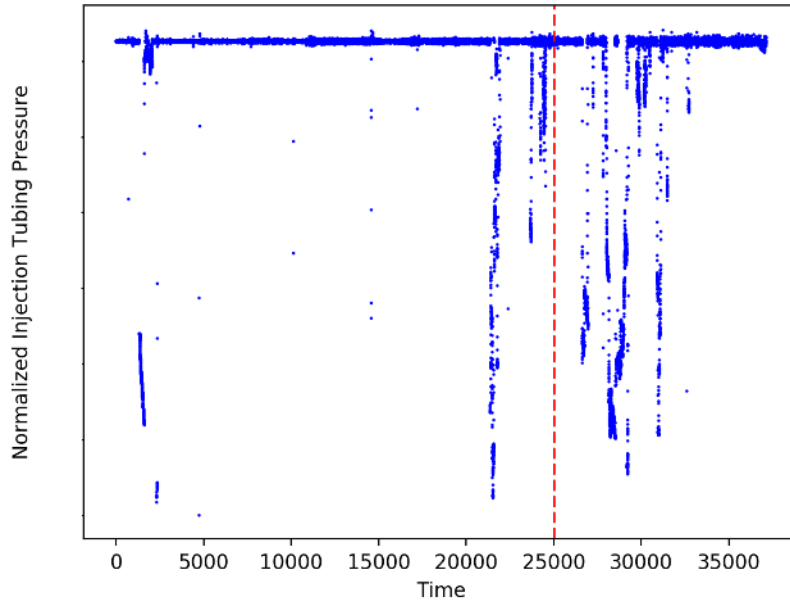


Figure 2.15: Trend of Injection Tubing Pressure

2.7 Conclusions

Machine learning can make use of complex industrial data for building data-driven models. The potential advantages of various machine learning methods under consideration have been discussed in this chapter. We have shown studies on two datasets. In the first dataset, the Deep Feedforward Neural Network has shown good predictive performance in capturing process trends. Also, the performances of ensemble decision tree based regression models are comparable. In the second dataset, all the built model have failed. We show that the model development task highlights the necessity of assessing data quality prior to model building. So, while applying machine learning to do data analytics in oil sands problems, data quality and priori knowledge play a vital role.

Chapter 3

Locally Weighted Quadratic Regression based Bayesian Optimization and its application in SAGD process

This chapter proposes the Locally Weighted Quadratic Regression based Bayesian Optimization (LWQRBO) method. This optimization algorithm inherits the Bayesian Optimization algorithm framework with Expected Improvement as the figure of merit for search. It utilizes locally weighted quadratic regression as the surrogate model. Further, the proposed LWQRBO is applied in a simulated SAGD process.

This chapter is organized as follows: Section 3.1 presents the brief review of literature on Bayesian Optimization. Section 3.2 revisits Efficient Global Optimization (EGO) and Locally Weighted Learning (LWL), and then proposes the Locally Weighted Quadratic Regression based Bayesian Optimization (LWQRBO). Next, two numerical cases are studied to test the proposed LWQRBO in Section 3.3. SAGD optimization literature review, problem description and the application of LWQRBO in SAGD process are discussed in Section 3.4. Conclusions are drawn in Section 3.5.

3.1 Literature Review of Bayesian Optimization

Derivative-free optimization (DFO) is of great importance in practical applications, and is necessary when the derivatives of the objective function are not available or

hard to compute, such as in the cases where the objective function is a computer simulation, a physical process or a complex mathematical function. DFO includes various classes of algorithms. For example, trust-region methods and Nelder-Mead simplex algorithm belong to local search methods, and multilevel coordinate search, branch-and-bound search and Response Surface methods belong to global search methods [43]. The well-known Mesh Adaptive Direct Search (MADS) is an extension of Generalized Pattern Search method [44], which also belongs to DFO. In this chapter, we are particularly interested in one of the subjects of DFO, Bayesian Optimization, which deals with optimizing black-box objective functions.

Jones et al. [45] proposed an Efficient Global Optimization (EGO) algorithm, which aims to optimize the black-box objective function by building the stochastic process response surface. Expected Improvement (EI) is used as the figure of merit which accounts for both the approximate function, and uncertainty of the surface. Maximization of EI yields a next sample point which is a trade-off solution to local and global search. Branch-and-bound algorithm is used to solve the sub-optimization problem - maximizing Expected Improvement. Gramacy et al. [46] proposed an algorithm to solve the optimization problem with black-box objective function and black-box constraints. To this end, the Augmented Lagrangian methods are applied to convert a constrained problem into an unconstrained problem, and the algorithm is integrated with Gaussian Process surrogate modelling, Expected Improvement and derivative-free methods [46]. Picheny et al. [47] included slack variables into Bayesian Optimization with the Augmented Lagrangian Framework, and also, the introduced slack variables are deployed to handle mixed constraints of equality and inequality, where they are treated as “joint” black-box.

There exist several variants of the EGO algorithm. Bootstrapped EI is proposed to estimate the variance of kriging model instead of classic EI in [48]. Further, multiple surrogate models are adapted into the EGO framework in [49]. In this work, at each optimization iteration, multiple sample points are obtained by maximizing EI for each of the surrogate models, rather than a single point from a single surrogate model.

In terms of application, Bayesian Optimization was proposed as a way to tune machine learning hyperparameters in [50]. Bayesian Optimization is related to surrogate model based black-box optimization.

Vu et al. [51] did a survey on surrogate model based black-box optimization. The work discusses multiple types of surrogate models, along with different merit functions and experiment designs. Also, entropy search is applied in Efficient Global Optimization in [52].

Talgorn et al. [53] applied locally weighted scatterplot smoothing for constructing a surrogate model, and therefore, to generate possible solutions. In their work, Mesh Adaptive Direct Search (MADS) is used to solve the black-box optimization problem with the built model. Also, the calculated shape parameter of weight function is selected by minimizing order error. Conn and Digabel combined MADS and quadratic models for black-box optimization [54]: The quadratic models are embedded into the MADS, and search and ordering strategies are performed with the models used in their work.

Dang approached the parameter tuning problem by considering it as a black-box optimization problem, and proposed an Optimization of Algorithms (OPAL) framework in [55]. This work also parallelized the OPAL framework and released a Python implementation.

An overview of existing surrogate model methods and the optimization framework, is given in [56], and also the usefulness of surrogate model based optimization for certain aerodynamic problem has been shown in [56]. The work by Koziel and Leifsson [57] includes an array of engineering applications of surrogate model based optimization. Furthermore, Mack et al. [58] applied the surrogate model optimization in an aerospace design problem.

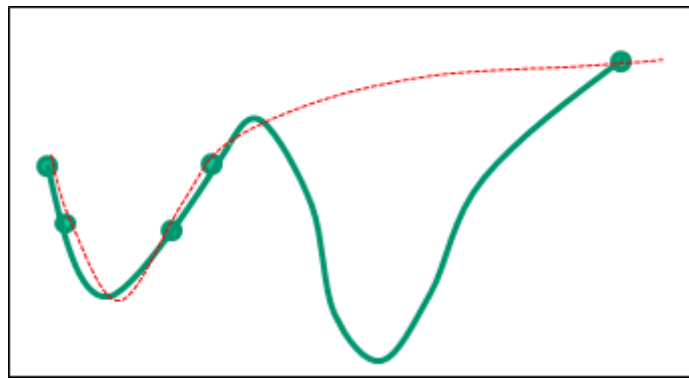
3.2 Locally Weighted Quadratic Regression based Bayesian Optimization

The Locally Weighted Quadratic Regression based Bayesian Optimization (LWQRBO) algorithm is proposed in this section. Prior to introducing LWQRBO, we describe its framework, the Efficient Global Optimization algorithm, in subsection 3.2.1. The surrogate modelling approach that is applied in this chapter, namely locally weighted learning, is introduced in subsection 3.2.2. Next, the proposed algorithm is described

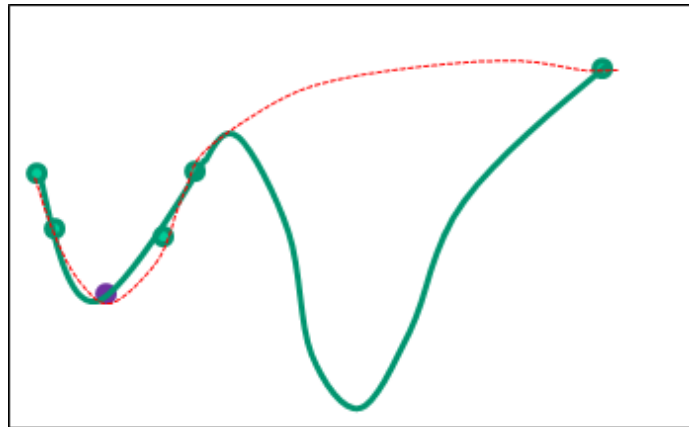
in detail in subsection 3.2.3.

3.2.1 Efficient Global Optimization

As discussed in Section 3.1, Bayesian Optimization includes a wide range of algorithms. We introduce its basic ideas and one of its representatives, the Efficient Global Optimization (EGO) which is proposed by Jones et al. [45]. We illustrate the sampling process in a one-dimensional case, by introducing a normal sample strategy followed by the sample strategy of Efficient Global Optimization. The introduction in this subsection is referenced from [45].



(a) Initial dataset and initially built surface



(b) Dataset and built surface in one iteration

The green points represent initial points sampled from the true curve, and the purple point denotes the calculated sampled point. The red dashed curve represents the built surface or the built surrogate model, and the green curve denotes the true function curve.

Figure 3.1: Sampling without considering model uncertainties

The first step is to build an initial surface with the initial dataset, and the initially built surface is represented by the red dashed line in Figure 3.1a. Then, the sample

point for the next iteration is calculated. Normally, the next sample point is calculated at the point, where it is the minimum of the initially built surface or the surface built in the previous iteration. In Figure 3.1b, purple dot indicates the sample point for next iteration. Next, this purple point is sampled from the true function, and the dataset is updated by adding the newly sampled point. Furthermore, surface is built with the new dataset, and is denoted by the red dashed line in Figure 3.1b. Finally, iterate until the stopping criteria is met.

However, we see from Figure 3.2 that there are model uncertainties, especially where the data are sparse. The black dashed lines represent the range of the uncertainties of the model.

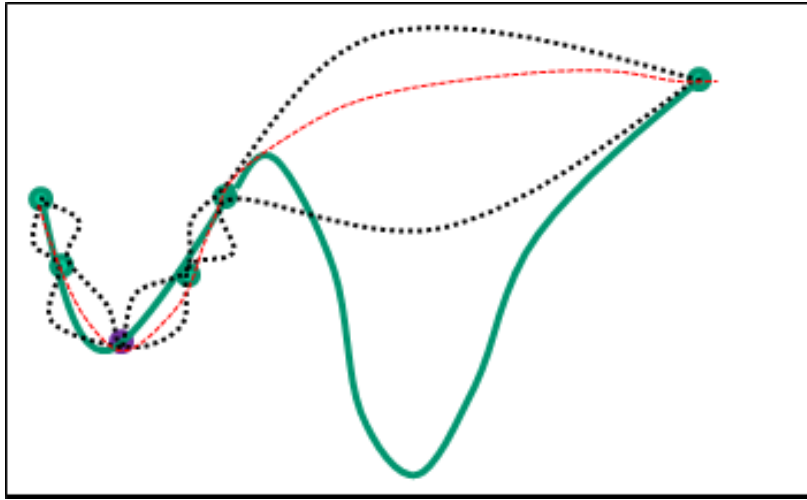


Figure 3.2: Model uncertainties

Bayesian Optimization considers the model uncertainties. There are many ways to consider model uncertainties, that is, many merit functions could be applied to determine the next sample point [50] [51]. Expected Improvement is one of them. Following the work by Jones et al. [45], Improvement and Expected Improvement can be defined as follows:

$$I(x) = \max(f_{min} - Y, 0) \tag{3.1}$$

$$E[I(x)] = E[\max(f_{min} - Y, 0)] \tag{3.2}$$

where f_{min} is the current minimum function value, and Y is the random variable to be minimized. A more specific expression of Expected Improvement is expressed in

Equation 3.3 [45]:

$$EI(x) = (f_{min} - \hat{y})\Phi\left(\frac{f_{min} - \hat{y}}{s}\right) + s\phi\left(\frac{f_{min} - \hat{y}}{s}\right) \quad (3.3)$$

where f_{min} is minimum function value. $\phi(\cdot)$ and $\Phi(\cdot)$ are the standard normal density and distribution functions, respectively. \hat{y} and s denote the prediction and standard error of prediction, respectively. From Equation 3.3, it can be seen that Expected Improvement considers not only model uncertainty but also information of the current minimum value and the built surface.

Efficient Global Optimization optimizes Expected Improvement to determine the next sample point. It normally applies branch-and-bound algorithm to maximize the Expected Improvement. It bounds the mean squared error via convex relaxation and bounds the prediction via nonconvex relaxation [45]. However, in this work, we use Genetic Algorithm to solve this problem, and the details of this will be presented in subsequent sections.

3.2.2 Locally Weighted Learning

Online prediction is required in industrial processes [59]; particularly, the online predictions of quality variables are important for monitoring, control and optimization of industrial processes. Considering that the process operation condition is changing, the predictive model should be updated [60]. Locally Weighted Learning (LWL) is one of the choices to build predictive models, and has been widely studied on its application in industrial process [59] [61]. Ge and Song [60] did a comparative study of locally weighted learning with SVR and PLS. The Locally Weighted Principal Component Analysis associated approaches are studied in [59] [62]. Also, locally weighted learning can handle missing data in industrial process [61]. A typical procedure of locally weighted learning can be summarized as follows [60] [63]:

1. A query point, q , comes;
2. Distance is calculated between the query point q and each point in the historical dataset;
3. Weight matrix of historical dataset is calculated via a weight function;
4. Do prediction with weighted dataset via a selected regression technique;
5. The built model is discarded. The system waits for the next query point.

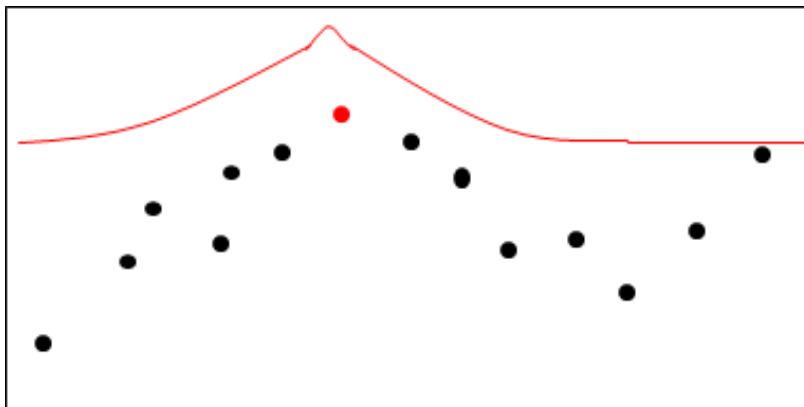


Figure 3.3: Illustration of locally weighted learning

In Figure 3.3, we illustrate the idea of locally weighted learning in a one-dimensional case. In this figure, the black points represent historical dataset, the red point denotes query point. The red line represents weights. It should be noted that if the data sample lies closer to the query point, it has larger weight. In other words, LWL selects the most relevant data to do regression, and the model is updated for each query point. Thus, it is useful in practice for chemical processes to account for the changing process operation conditions. Also, the locally weighted model can deal with nonlinearity [63]. Therefore, locally weighted regression is applied as the surrogate model in the Bayesian Optimization framework. Specifically, locally weighted quadratic regression is considered.

Next, we introduce Equation 3.4 and Equation 3.5, from [63]. These equations are related to least squares algorithms of locally weighted linear models. Equation 3.4 is the prediction expression at the point q of local linear models, and Equation 3.5 is the variance of the prediction at q of local linear models.

$$\begin{aligned}
 \hat{y}(q) &= q^T (Z^T Z + \Lambda)^{-1} Z^T W y \\
 &= S_q^T y \\
 &= \sum_{i=1}^N s_i(q) y_i
 \end{aligned} \tag{3.4}$$

where q is the point we want to predict, $Z = WX$ and W denotes weight matrix. X and y denote inputs and output of the dataset, respectively. Λ is a diagonal matrix

with small positive diagonal elements to avoid singular matrix.

$$Var(\hat{y}(q)) = \sum_i s_i^2(q) \sigma^2(x_i) \quad (3.5)$$

where $s_i(q)$ comes from Equation 3.4 and $\sigma(x_i)$ denotes the standard deviation of random noise at point i . The above two equations will be modified to be incorporated into Expected Improvement. The details will be introduced in next section.

3.2.3 Locally Weighted Quadratic Regression based Bayesian Optimization

First, the prediction expression of locally weighted quadratic regression must be obtained. The quadratic terms in quadratic regression could be regarded as regressors of linear regression. Consider a two-dimensional case. For other dimensions, it can be modified accordingly. The inputs, $X_{input} = [X_1, X_2]$, are expanded to $X = [X_1, X_2, X_1^2, X_2^2, X_1X_2]$ as the regressors to perform quadratic regression. X will be weighted to Z by $Z = WX$. Z will be used in the general locally weighted linear regression expression in Equation 3.4. Also, considering that solving the inverse of a matrix may suffer from the singular matrix problem, we choose stable numerical algorithms to solve the inverse of a matrix, and therefore, we set the diagonal elements in Λ matrix to zero. So, the prediction at point q using locally weighted quadratic regression is:

$$\begin{aligned} \hat{y}(q) &= q^T (Z^T Z)^{-1} Z^T W y \\ &= S_q^T y \\ &= \sum_{i=1}^N s_i(q) y_i \end{aligned} \quad (3.6)$$

As noted previously, Expected Improvement relies on prediction and standard error of the prediction. Besides the prediction term, we also need the standard error of prediction. For simplicity, we start the analysis without considering the random noise. For this case, Equation 3.5 can be expressed as:

$$Var(\hat{y}(q)) = \sum_i s_i^2(q) \quad (3.7)$$

Therefore, from Equation 3.6 and Equation 3.7, the variance of prediction at point q of the locally weighted quadratic regression can be rewritten as:

$$\begin{aligned}
Var(\hat{y}(q)) &= \sum_i s_i^2(q) \\
&= S_q^T S_q \\
&= q^T (Z^T Z)^{-1} Z^T W (q^T (Z^T Z)^{-1} Z^T W)^T \\
&= q^T (Z^T Z)^{-1} Z^T W W^T Z (Z^T Z)^{-1} q
\end{aligned} \tag{3.8}$$

Also, the standard error at the point of q of a locally weighted quadratic regression is expressed in Equation 3.9:

$$\begin{aligned}
std(\hat{y}(q)) &= \sqrt{Var(\hat{y}(q))} \\
&= \sqrt{q^T (Z^T Z)^{-1} Z^T W W^T Z (Z^T Z)^{-1} q}
\end{aligned} \tag{3.9}$$

where $X = [X_1, X_2, X_1^2, X_2^2, X_1 X_2]$, $Z = WX$, and $W = f_w(X, q)$. There are many ways to choose the weight function, f_w , and the distance, d . We choose the exponential function as the weight function and Euclidean distance as the distance measure. Mathematically, they are defined as [63]:

$$f_w = k e^{-d/l} \tag{3.10}$$

where d is Euclidean distance, k and l are function parameters. The distance between x_q and x_i is:

$$d = \sqrt{(x_q - x_i)^T (x_q - x_i)} \tag{3.11}$$

This proposed LWQRBO algorithm solves optimization problems whose objective function is a black-box function, with bound constraints on the decision variables. We consider solving a minimization problem. We first introduce the steps of LWQRBO, which inherits the framework of Efficient Global Optimization from [45]. We use a 1-d case with 3 initial points to describe it:

Steps:

1. Provide initial points (x_1, x_2, x_3) for the optimization algorithm, and sample from the true black-box function to calculate (y_1, y_2, y_3) .
2. Build surrogate model f_s , with locally weighted quadratic regression, on the initial dataset $[(x_1, y_1), (x_2, y_2), (x_3, y_3)]$. $y_{min} = \min(y_1, y_2, y_3)$, assume $x_{min} = x_3$.

3. Calculate the prediction \hat{y} , and the standard error of prediction std , of the built surrogate model (i.e., locally weighted quadratic regression model), at the query point q .

4. Maximize the Expected Improvement to find the next point to sample, x_4 .

5. If y_4 is less than y_{min} , set $y_{min} = y_4$ and $x_{min} = x_4$; Otherwise, retain y_{min} and x_{min} ; Then, update the dataset by appending new sample point and get $[(x_1, y_1), (x_2, y_2), (x_3, y_3), (x_4, y_4)]$.

6. If stopping criteria are met, (i.e., EI satisfying the prescribed threshold value, or the maximum number of iterations reached), the algorithm stops. The solution is x_{min} , with the objective function value y_{min} . Otherwise, repeat Step 2 to Step 6 with the appended dataset.

Now, let us see the specific details of the proposed algorithm, LWQRBO. In this work, to use locally weighted quadratic regression as the surrogate model, suitable modifications are made to the EGO framework. Analysis and explanation are also described for applying locally weighted quadratic regression in this framework. Specific details of the algorithm are as follows:

Providing Initial Dataset

Latin hypercube sampling is applied to provide the initial points [45], and the number of sampled points is around $10p$, where p is the dimension of the function inputs, or variables of the surrogate model [45]. p is also the number of decision variables of the optimization algorithm. After sampling from the true black-box function with initial points to obtain corresponding outputs, the initial dataset have been constructed.

Preparing for Expected Improvement

Calculate the prediction $\hat{y}(q)$ with Equation 3.6, and the standard error of prediction $std(q)$ with Equation 3.9, at the new point q , or called query point, with locally weighted quadratic regression. These are used for the calculation of Expected Improvement.

Calculating Expected Improvement

Calculate Expected Improvement, by replacing \hat{y} and s in Equation 3.3, with E-

quation 3.6 and Equation 3.9, respectively. The estimation of Expected Improvement at point q of a locally weighted quadratic regression could be written as:

$$EI(q) = (f_{min} - q^T(Z^T Z)^{-1}Z^T W y) \Phi\left(\frac{f_{min} - q^T(Z^T Z)^{-1}Z^T W y}{\sqrt{q^T(Z^T Z)^{-1}Z^T W W^T Z(Z^T Z)^{-1}q}}\right) + (\sqrt{q^T(Z^T Z)^{-1}Z^T W W^T Z(Z^T Z)^{-1}q}) \phi\left(\frac{f_{min} - q^T(Z^T Z)^{-1}Z^T W y}{\sqrt{q^T(Z^T Z)^{-1}Z^T W W^T Z(Z^T Z)^{-1}q}}\right) \quad (3.12)$$

where f_{min} is the current best function value. $\phi(\cdot)$ and $\Phi(\cdot)$ are the standard normal density and distribution functions, respectively. X and y denote input and output, respectively. q is the unknown point or query point. W is weight matrix calculated by weight function shown in Equation 3.10. Z is the weighted matrix of X .

Maximizing EI

In Step 4, we want to maximize $EI(q)$ to find the next sample point. It is a sub-optimization problem, and we provide a description of the solution below.

First, it consists of probability density and distribution function. Second, we consider it in view of modelling: Assume we have training data and testing data, and will make predictions for all the inputs in testing data. Locally weighted learning has different model parameters for different inputs of testing data, with the same training data. Because it builds a model for each input in test data, implying W and Z in Equation 3.12 could be different for different data points to be predicted. Additionally, W and Z are unknown, and are functions of q .

Equation 3.12 is therefore a highly non-linear and complex function with respect to q , and is hardly tractable analytically. Hence, Genetic Algorithm is applied to solve this sub-optimization problem.

Stopping Criteria

If the stopping criteria are not met, the dataset is updated by adding the obtained query point q and its function value, y_q , sampled from the true black-box function. Then, we use locally weighted quadratic regression in next iteration with the updated dataset to build the model. Otherwise, it stops. The stopping criteria is controlled by the following:

1. If the Expected Improvement is less than a specified percentage, p_1 , of the

current minimum value f_{min} , it stops;

2. If the new sampled objective function value is less than a specified percentage, p_2 , of the current minimum value, it stops;

3. If the number of iterations, or black-box calculations exceeds maximum calculations M , it stops.

All of the above stopping criteria could be used in the algorithm. The mode of each criterion can be adjusted accordingly in practice. Criteria 1 and 2 allow the optimization algorithm to explore more of the optimum and Criterion 3 controls the calculation time.

Figure 3.4 presents the flowchart of the proposed approach. The main modifications in the existing framework are highlighted in boldface.

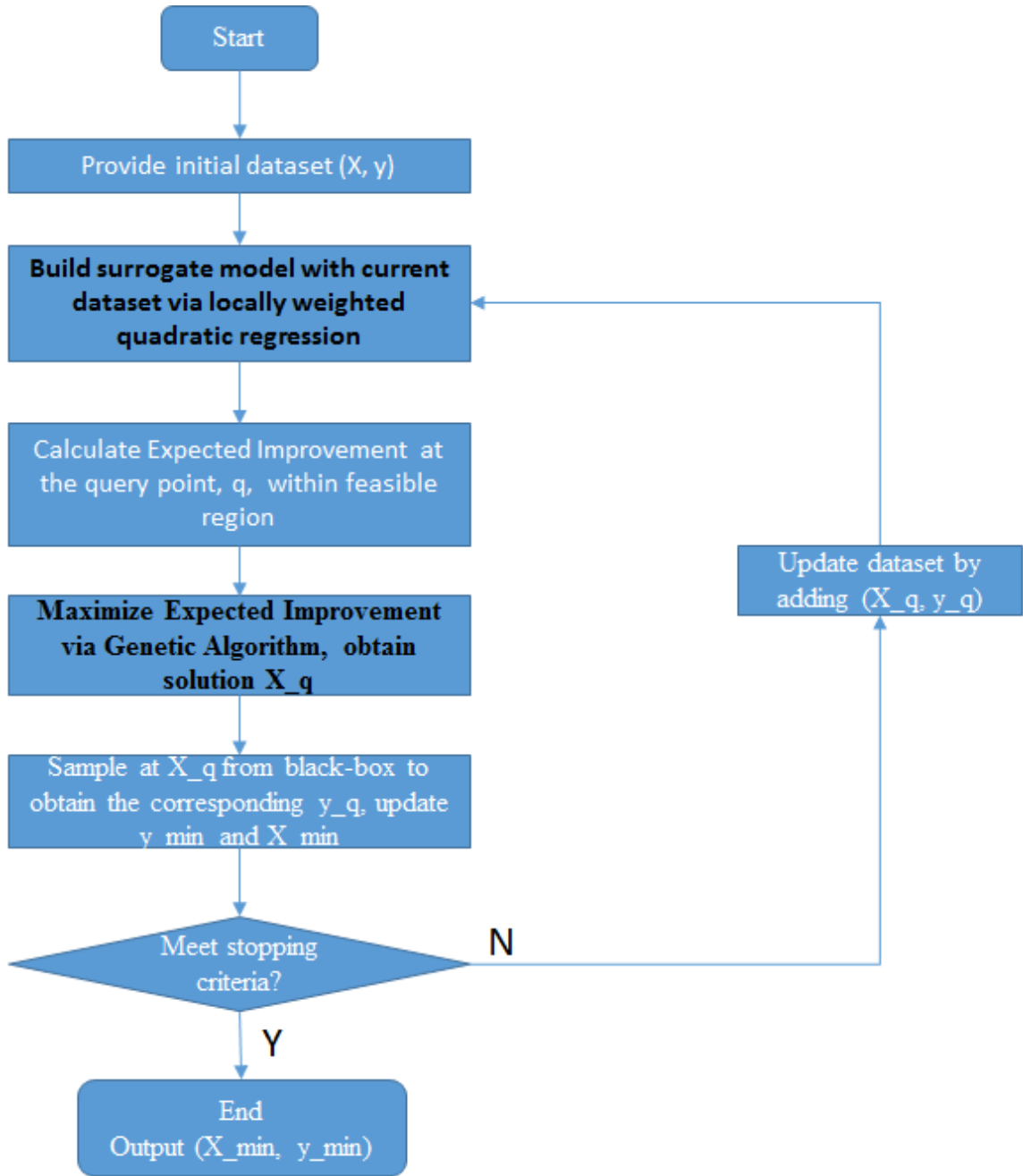


Figure 3.4: Flowchart of LWQRBO

3.3 Case Study

In this section, we present the validation results of Locally Weighted Quadratic Regression based Bayesian Optimization (LWQRBO) in two numerical test functions.

3.3.1 Case Study 1

In this subsection, we apply the Bayesian Optimization with locally weighted quadratic regression algorithm in a one-dimensional numerical test function, as given in Equation 3.13:

$$y = \frac{x}{10} \sin\left(\frac{\pi}{2}x\right) \quad (3.13)$$

where $x \in [1, 10]$.

Figure 3.5 shows the true curve of this test function as the black line. It has one global minimum and several local minima. Latin hypercube sampling is applied to sample the 10 initial data points, which are marked in the figure by blue markers. The initial data points are distributed across the range $[1, 10]$ almost evenly. Red points represent the sampled points calculated by the optimization algorithm. We see that most of the sampled points are clustered around the global minimum.

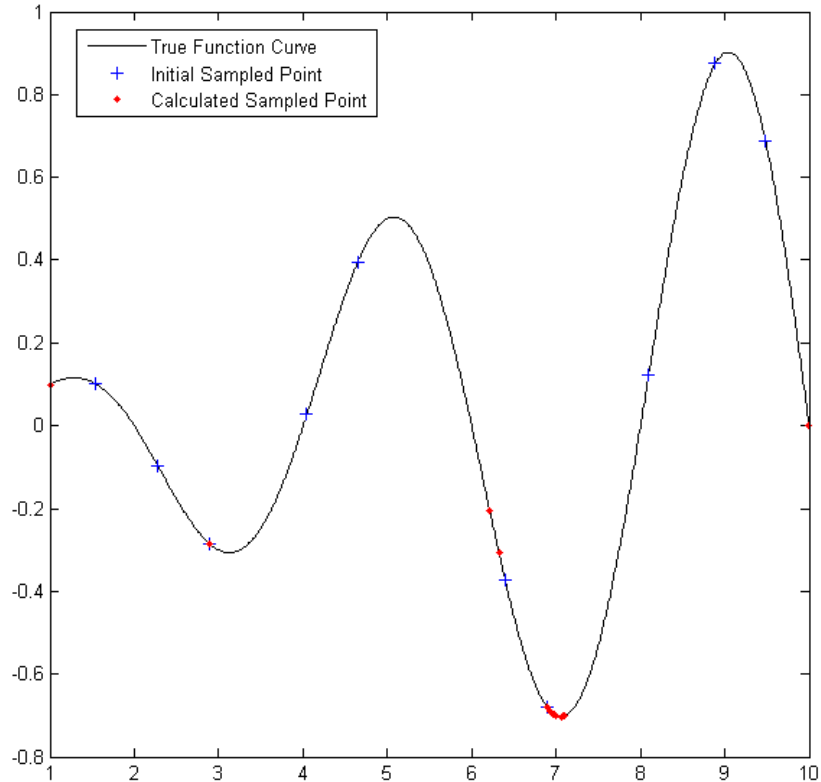


Figure 3.5: Curve of 1-d test function

Figure 3.6 shows the performance of optimization algorithm through iterations. The red line represents the sampled function value and blue line represents the current calculated minimum, also called the best calculated value until the current iteration. We see that the blue line gradually converges to the global minimum.

The algorithm samples where the Expected Improvement is maximized. As discussed before, Expected Improvement takes both model uncertainty and optimization into consideration. It is not necessary that the function value of the sampled point in next iteration is lower than that in the current iteration. Because the sampled points not only consider exploring the minimum in next iteration but also consider model uncertainty to make the built surface more accurate. The current minimum value is updated during the iterations in the optimization algorithm, and therefore keeps decreasing.

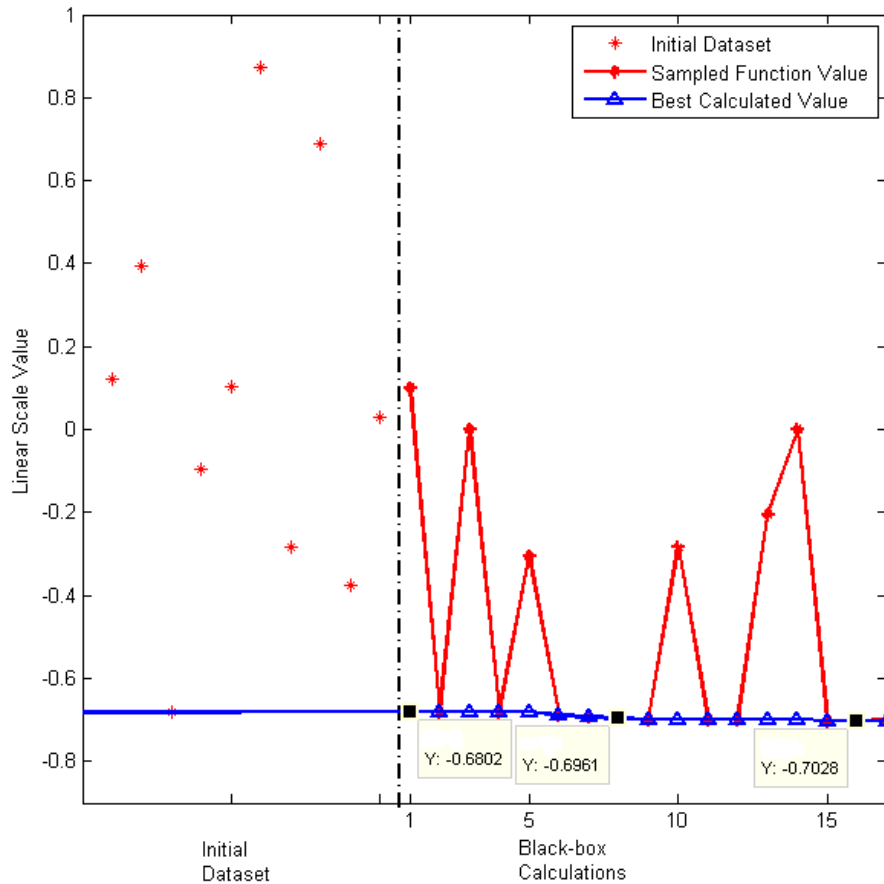


Figure 3.6: Performance through iterations

The dashed vertical line marks a separation between the initial dataset and newly found sample points as the optimization process progressed. It shows that the minimum finally found is not the minimum in initial dataset, which also demonstrates this sampling algorithm indeed works.

Expected Improvement is maximized at each iteration to determine the next sample point. Figure 3.7 shows iterative trend of the Expected Improvement.

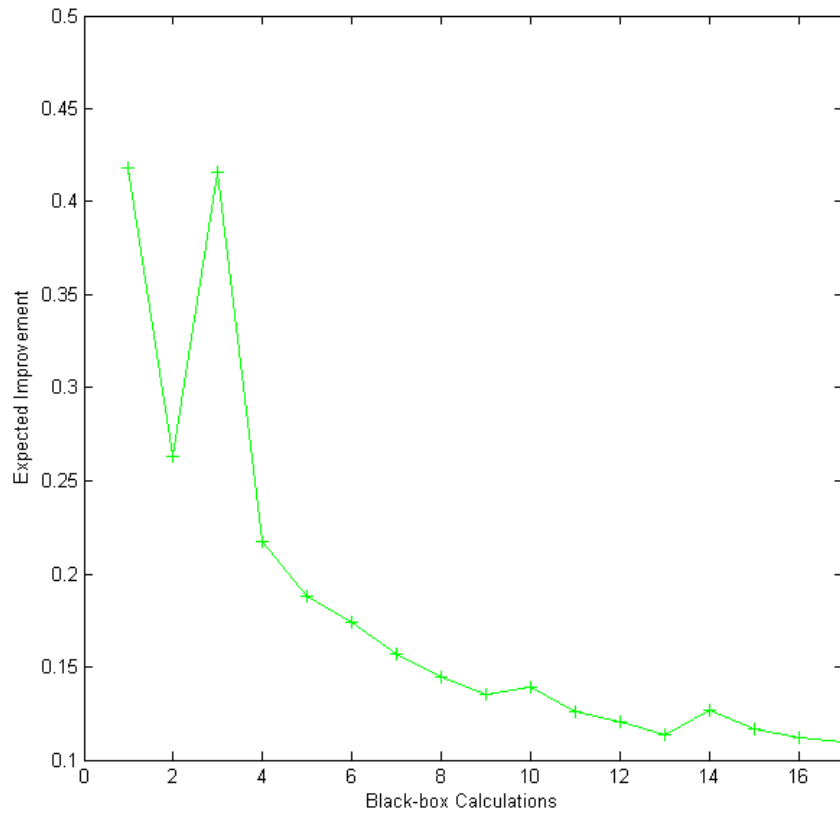


Figure 3.7: Expected Improvement of 1-d case

3.3.2 Case Study 2

The proposed algorithm is also tested in a 2-dimensional numerical function, called Branin function.

The Branin function is expressed in Equation 3.14 [64]:

$$y = a(x_2 - bx_1^2 + cx_1 - r)^2 + s(1 - t)\cos(x_1) + s \quad (3.14)$$

where we choose the following settings:

$a = 1$, $b = \frac{5.1}{4\pi^2}$, $c = \frac{5}{\pi}$, $r = 6$, $s = 10$ and $t = \frac{1}{8\pi}$. $x_1 \in [-5, 10]$ and $x_2 \in [0, 15]$.

For those settings, the function has 3 global minima:

The function value is $f(x^*) = 0.397887$, at $x^* = (-\pi, 12.275)$, $(\pi, 2.275)$ and $(9.42478, 2.475)$ [64].

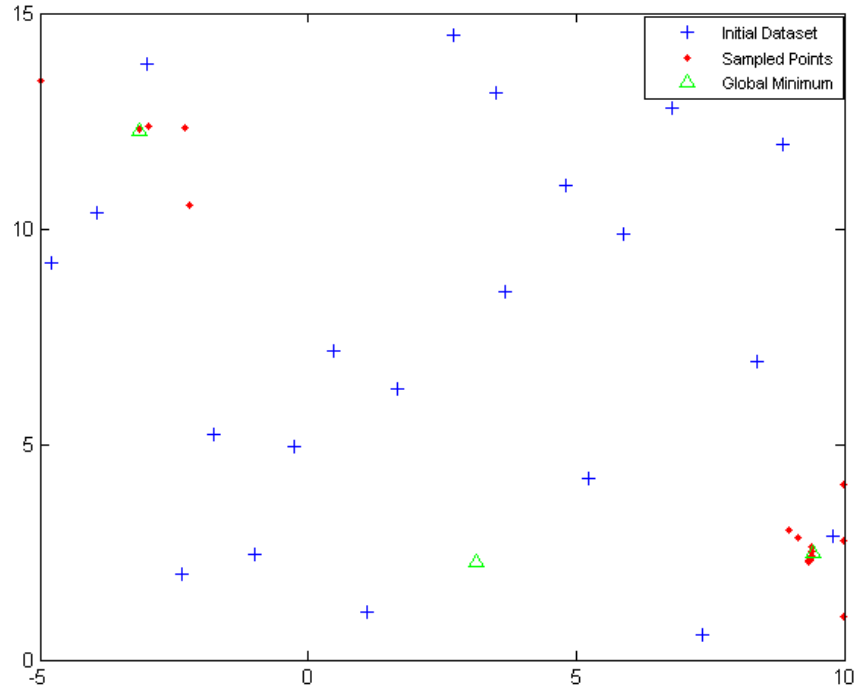


Figure 3.8: Locations of sampled points

Figure 3.8 shows locations of the sampled points. The 21 initial data points are distributed in the square range and are denoted by blue markers. Three green triangles represent locations of the three global optima. Red points represent the points obtained by maximizing EI. We see that most points sampled during iterations are around two of the three global optima, $x^* = (-\pi, 12.275)$ and $(9.42478, 2.475)$.

Figure 3.9 illustrates the performance of LWQRBO on the Branin test function. As discussed before, we know the function value of the sampled points during iterations are regarded as candidates of the final optima, since maximizing EI considers the trade-off between surface optima exploitation and consideration of model uncertainty. Therefore, the algorithm does not guarantee its continuous decrease. Moreover, we see that the current calculated minimum (blue line) converges to global optimum gradually, from 0.3985, 0.3983 to 0.3981. The obtained optimal point is located at $(-3.1477, 12.2983)$, which is very close to $(-\pi, 12.275)$, as seen in Figure 3.8.

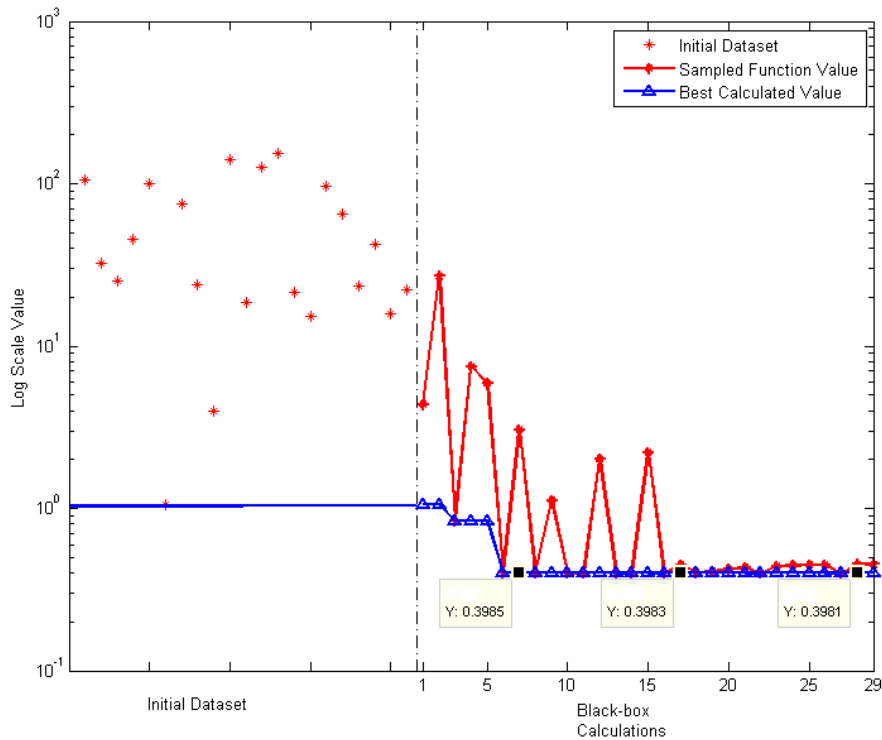


Figure 3.9: Performance through iterations

Points to the left of the vertical line are the initial dataset, and those to the right are the points determined as the optimization process progressed. The vertical axis

is log scaled for the purpose of a clear view; otherwise, the curve decreases quickly and steeply in linear scale.

Expected Improvement is maximized to calculate the next sample point. Figure 3.10 shows the trend of Expected Improvement through iterations.

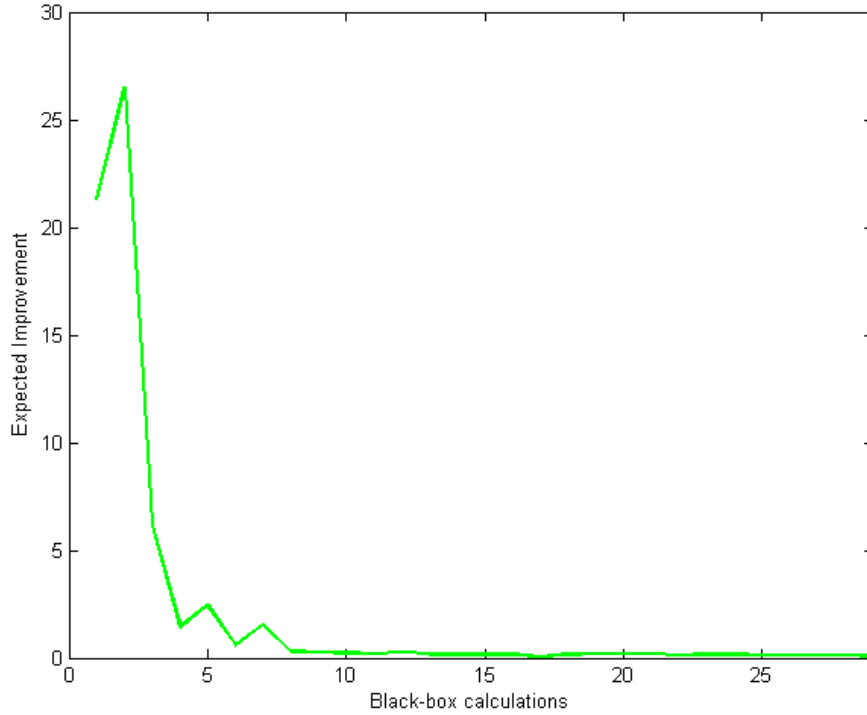


Figure 3.10: Expected Improvement of 2-d case

3.4 Application in simulated SAGD process

In this section, Locally Weighted Quadratic Regression based Bayesian Optimization (LWQRBO) is applied to a simulated SAGD process. In subsection 3.4.1, a literature review of SAGD optimization is provided. The motivation and description of the problem are formulated in subsection 3.4.2. In subsection 3.4.3, optimization results are presented.

3.4.1 SAGD Optimization Review

SAGD is an efficient approach to extract bitumen from reservoir from an economic point of view [65], and it has been extensively used to produce bitumen, especially in Alberta, Canada. The optimization solutions of SAGD can help engineers with the decision-making process [66].

SAGD production can be enhanced with first principle knowledge and therefore, there are many variants [67]. One approach to improve SAGD is to design the injected steam. Two well-known variants of this type are Steam and Gas Push (SAGP), and Expanding Solvent SAGD (ES-SAGD) [67] [68]. SAGP injects steam with non-condensed gas, such as nitrogen or natural gas; ES-SAGD injects steam with solvent [68]. Also, an elaborate design of the SAGD facilities, especially the well design, improves SAGD efficiency. The effect of well design, such as lengths, liner and tubing, wellbore annulus on SAGD performance has been discussed in [69]. Furthermore, in the cases where reservoirs are very thin, one-well SAGD [67] could be considered as a candidate.

Steam injection strategy plays an essential role in SAGD optimization. Optimizing SAGD by adjusting steam injection pressure with a reservoir simulation model is studied in the work by Card et al. [5]. In the study by Gates et al. [70], optimization is also performed by adjusting injection pressure. Also, the role of steam injection strategy in determining the performance of SAGD is described in [71] and [72].

Optimizing economic performance of SAGD is a main focus. There are many economic performance measurements of the SAGD process, such as Steam to Oil Ratio (SOR), cumulative Steam to Oil Ratio (cSOR), Net Present Value (NPV), etc. The economic performance measurement to use depends on the problem being investigated. For example, the work of [70] studies optimization of cSOR via Genetic Algorithm, and Net Present Value (NPV) is considered as an objective to be optimized in [71]. Other economic performance measurements, such as Internal Rate of Return (IRR) and Pay Back Period (PBP) are studied in [65].

Uncertainty is another research topic while doing optimization in SAGD. The study in [71] considers the uncertainty of the economic forecast when optimizing the SAGD process, and Monte Carlo simulation is used to quantify uncertainty in

this work. Uncertainty also arises from reservoir geological properties. In [73], a SAGD optimization workflow is presented to capture the geological uncertainties. Another study [74] proposes to reduce reservoir geological property uncertainties using a mixed-integer linear optimization-based method.

Surrogate model based optimization in SAGD also receives a variety of research focuses. Work by Mohaghegh et al. [4] introduces the development of Surrogate Reservoir Modelling. In [75], Polynomial model and Kriging model are constructed as proxy models, then the gradient based algorithm is applied for optimization. Yang et al. [71] have built polynomial response surface for NPV to perform an economic optimization of SAGD. Besides, Network-based efficient global optimization (NEGO) method is applied to optimize the SAGD process in [76].

We learn from the above review that SAGD optimization could be conducted using various methods. Readers are referred to [3] for more information. This section aims to optimize the SAGD process. More details are introduced in the next subsections.

3.4.2 Motivation and Problem Description

To optimize SAGD, we need to build an optimization model. An optimization model consists of three main elements: objective function, decision variables and constraints. We introduce and discuss each element in detail below.

From Section 3.4.1, we know that there are many metrics measuring the performance of SAGD process, such as Steam to Oil Ratio (SOR), cumulative Steam to Oil Ratio (cSOR), Net Present Value (NPV), etc. In this study, SOR is utilized as the objective function to be optimized.

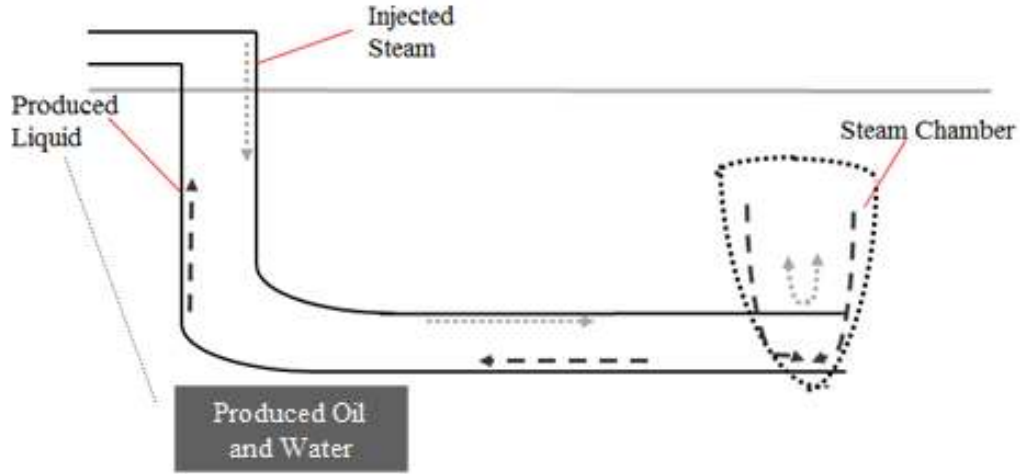


Figure 3.11: Schematic of SAGD process

Figure 3.11 shows a schematic of the SAGD process. We see that the produced liquid consists of oil and water. SOR is calculated as the ratio of the injected steam flowrate to the produced oil flowrate, as follows:

$$SOR = \frac{\text{Flowrate of Injected Steam}}{\text{Flowrate of Produced Oil}} \quad (3.15)$$

From Equation 3.15, we know that a smaller value of SOR means more produced oil with less injected steam, while a larger SOR value means more injected steam with less produced oil. To optimize the SAGD process performance measured by SOR, we need to minimize SOR. However, the mathematical function describing the relationship between SOR and other process variables is not available. Therefore, we regard the objective function as a black-box function.

Also, from [5], [70], [71] and [72], it is learned that steam injection strategy plays a core role in the performance of SAGD process. Thus, we focus on optimizing SOR by determining the optimal injected steam operating point. Specifically, flowrate and pressure of the injected steam are regarded as decision variables. They are operational variables, and could be manipulated or controlled in practice according to the feasible solution of the optimization model.

Those manipulated variables have operational ranges in practice for the purpose of safety, and those upper and lower bounds of the process variables are constraints in this optimization problem.

The specific description of the three elements of the optimization model is shown in Figure 3.12.

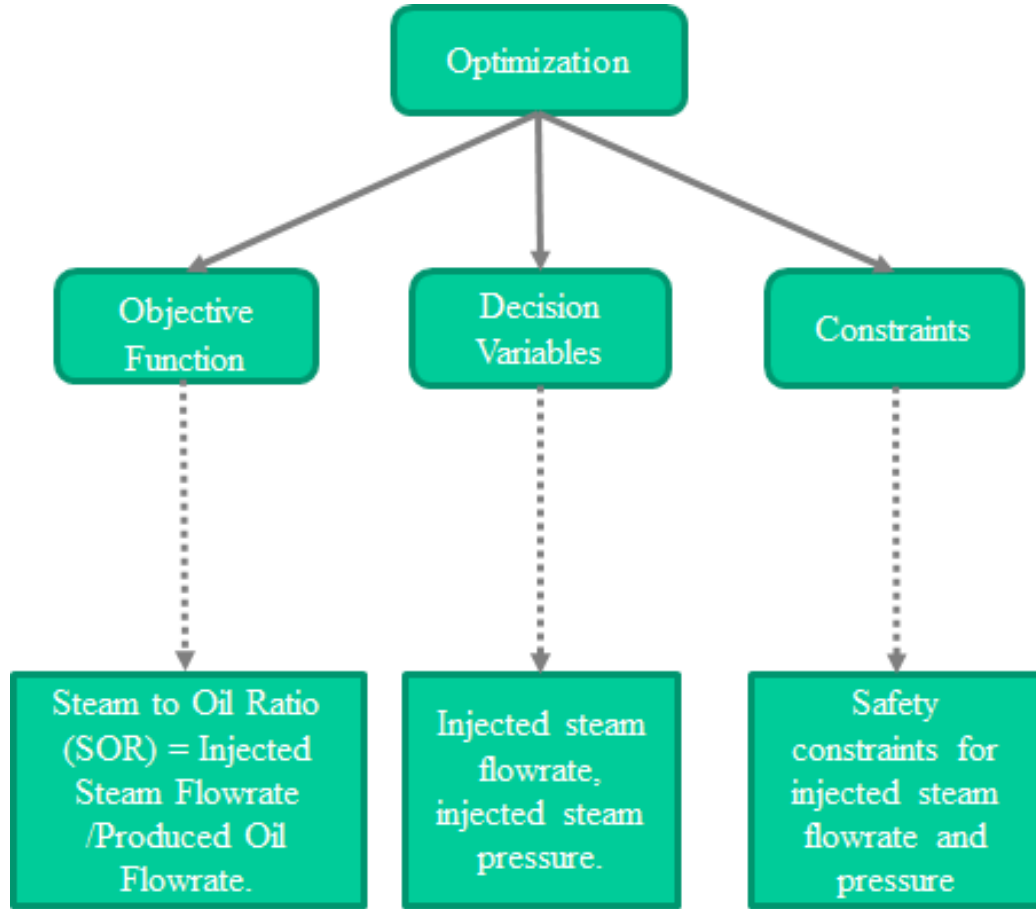


Figure 3.12: Optimization model elements

With the above analysis, the optimization model could be written as:

$$\begin{aligned}
 & \underset{x_{IF}, x_{IP}}{\text{minimize}} && f_{SOR}(x_{IF}, x_{IP}) \\
 & \text{subject to} && \\
 & && x_{IF} \leq U_F \\
 & && x_{IP} \leq U_P \\
 & && x_{IF} \geq L_F \\
 & && x_{IP} \geq L_P
 \end{aligned} \tag{3.16}$$

where x_{IF} and x_{IP} denote the injected steam flowrate and injected steam pressure, respectively. U_F and L_F denote the upper and lower bounds of the injected steam

flowrate, separately. U_P and L_P denote the upper and lower bounds of injected steam pressure, separately.

The purpose is to identify an optimal operation condition, which will generate the corresponding optimal SOR of the SAGD process. The proposed LWQRBO algorithm in this chapter is applied to solve this optimization problem.

In LWQRBO, maximizing EI is utilized to find the point which is able to improve the objective function value most probably, with the uncertainties in the surrogate model being considered. The surrogate model constructed here is an approximation of the black-box function (a real process in this work) that we want to learn. If the relationship between inputs and output changes over time, EI cannot capture the uncertainties in the surrogate model, which models the black-box objective function.

We therefore target this case in SAGD process: the function of SOR with respect to injection flowrate and injection pressure is static. That is, if given the same inputs (injected flowrate and pressure), the process will respond and generate the same SOR. In this case, other variables of SAGD may contain dynamic relationships, but the static relationship between SOR and injection flowrate as well as injection pressure holds. In this period, the black-box function to be optimized is a static time-invariant function, and therefore, we could apply LWQRBO to sample from the real process.

Considering the optimization algorithm to sample from real process, we see the following difference from sampling from a numerical function:

1. Historical dataset plays the role of initial points.
2. Sampling a real process at different time instances plays the role of different iterations in the optimization algorithm.

3.4.3 Optimization Results

In this subsection, we show the SAGD optimization results obtained using the LWQRBO method. Some of the main parameters of the reservoir are listed in Table 3.1.

Table 3.2 lists the operational upper and lower bounds of the injection flowrate and injection pressure in this case study.

Figure 3.13 shows the procedure of the optimization algorithm. 21 historical data points are provided as initial data in this problem. After building the initial

Table 3.1: Reservoir Parameters

Parameter Name	Value
Well length (m)	250
Heat transfer coefficient of the liquid pool ($W/m^2/K$)	$0.5 * 10^6$
Latent heat of steam vaporization (J/kg)	$780 * 10^3$
Reservoir temperature ($^{\circ}C$)	4
Thermal diffusivity of reservoir (m^2/s)	$6.4467 * 10^{-7}$
Porosity of formation	0.35
Oil saturation	0.85
Steam quality	0.95

Table 3.2: Operational Bounded Constraints

Parameter Name	Value
Upper Bound of Injection Flowrate (lb/s)	7
Lower Bound of Injection Flowrate (lb/s)	1
Upper Bound of Injection Pressure (psi)	2200
Lower Bound of Injection Pressure (psi)	1500

surrogate model, the sampled point in next iteration is found by maximizing Expected Improvement. The red line represents the sampled function value (real value of SOR with respect to the sampled input), which is generated from the real process, and the blue line represents the optimal value obtained up to the current iteration. Every time the algorithm samples from the process, the dataset is updated.

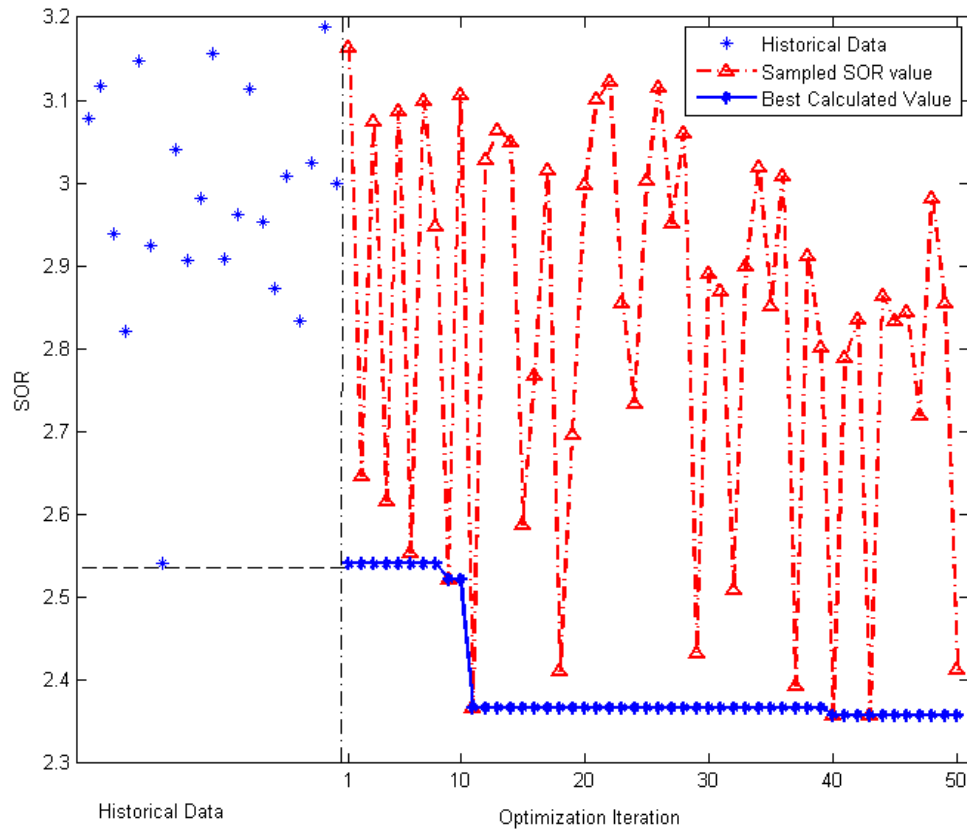


Figure 3.13: SAGD Optimization performance

As discussed in Section 3.3, the sampled points of input are just candidate solutions for the optimal value, and the sampled function value does not need to be less than that in the previous iteration. The blue line shows that the current minimum decreases during the iterations of the optimization algorithm.

All iterations shown above in Figure 3.13 solve one optimization problem. The optimization algorithm ends after the 50th iteration and the optimal SOR is found as 2.358. The corresponding input, the injection flowrate being 1 lb/s and the injection pressure being 1500 psi, will be implemented in the real process. Figure 3.14 shows the trend of Expected Improvement iteratively.

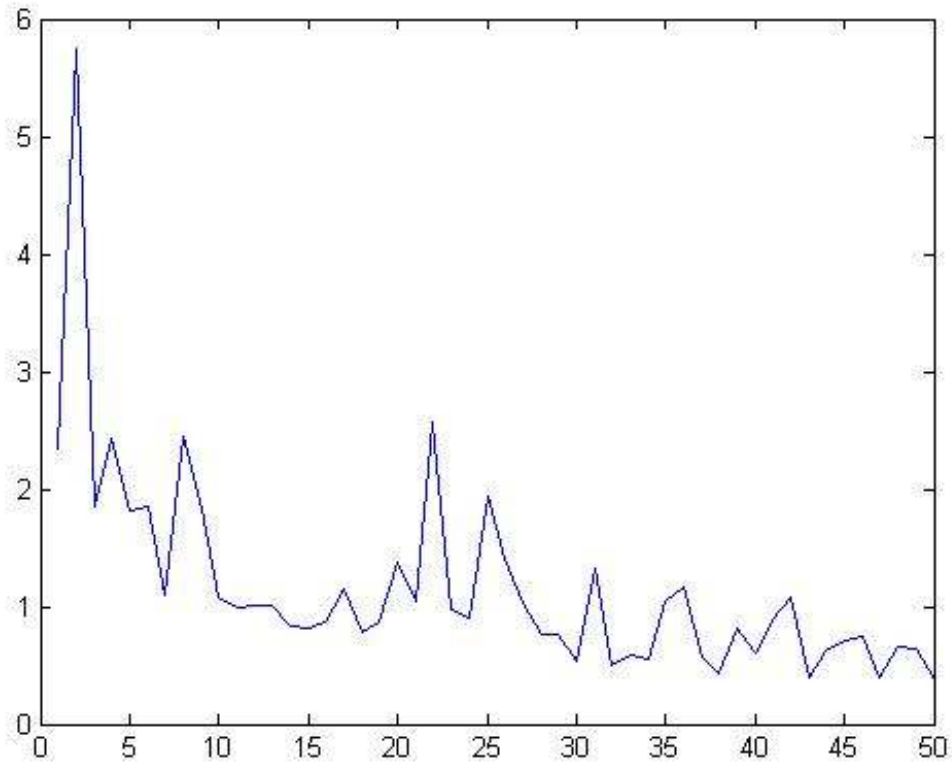


Figure 3.14: Trend of Expected Improvement

Figure 3.15 shows the location of initial data points and the sampled data points within the given operational region. Initial data points are denoted by the circles. The solid points represent the sampled points in the optimization algorithm, and are located both inside the region and along the edges. It demonstrates that the optimization algorithm does not search in a local neighborhood only. Instead, it also samples where the data are more sparse and where the model is more uncertain, which can be observed from the lower region of the left edge and the upper region of the right edge. Finally, it locates the optimum at $(1, 1500)$, which is the lower left corner.

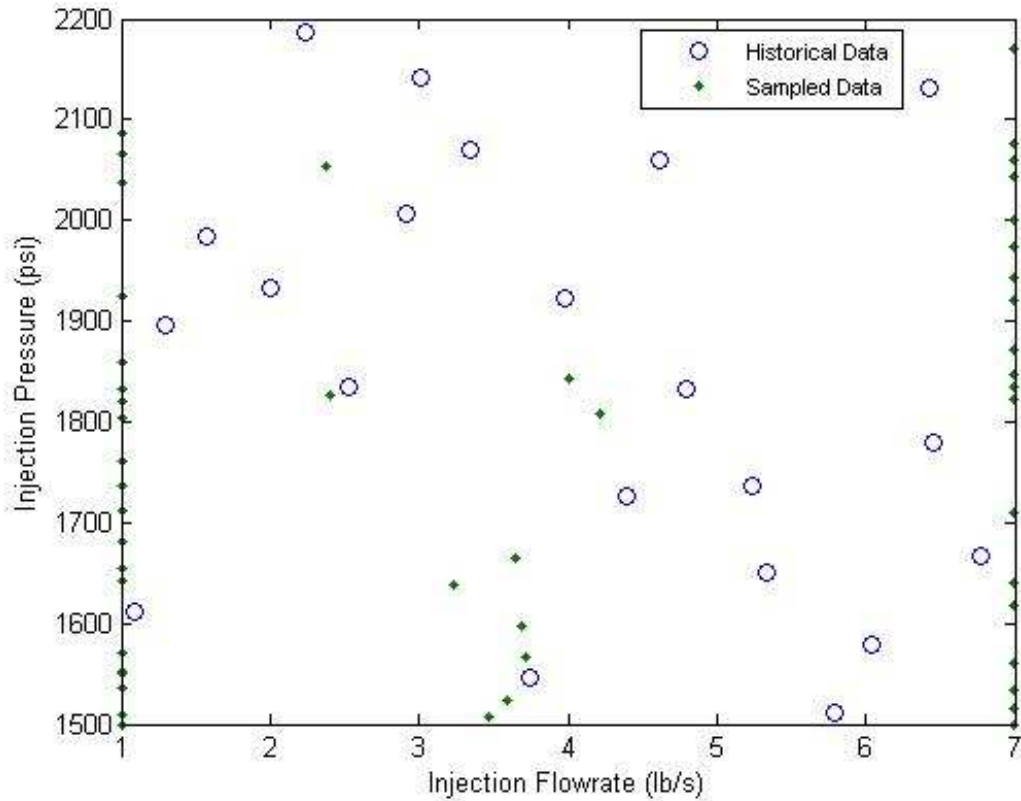


Figure 3.15: Location of Initial Data and Sampled Data

3.5 Conclusions

In this chapter, Locally Weighted Quadratic Regression based Bayesian Optimization (LWQRBO) is proposed. The literature review includes Bayesian Optimization and related research subjects, such as Derivative-free Optimization and Surrogate Model based Black-box Optimization. Efficient Global Optimization and Locally Weighted Learning are introduced prior to the introduction of the proposed approach for making the procedures of LWQRBO easy to understand. Two numerical test functions are applied to test the performance of the proposed approach. LWQRBO is also applied in a simulated SAGD process to optimize SOR by determining the optimal injection steam operational points. The proposed LWQRBO algorithm demonstrates its usefulness in SAGD process.

Chapter 4

Stacking online soft sensor application in SAGD process

In this chapter, a stacking online soft sensor that is applicable for monitoring purposes is designed for the SAGD process. The literature review of soft sensor design approaches is included in Section 4.1. The proposed online soft sensor approach is inspired by stacking models, so a brief review of stacking models is included in Section 4.2. Next, three popular models in soft sensor applications, Partial Least Squares Regression (PLSR), Gaussian Process Regression (GPR) and Support Vector Regression (SVR), are introduced in Section 4.3 and they are applied as offline predictive models. In Section 4.4, the proposed stacking online soft sensor and its feasibility are described in detail. Two case studies are shown in Section 4.5. Conclusions to this chapter are provided in Section 4.6.

4.1 Review of soft sensor design approaches

Soft sensors are useful in the monitoring of industrial processes [77] [78] [79]. For example, they are applied to predict the process variables which are difficult to measure online, such as the water content of the produced liquid of SAGD process. They are also alternatives to expensive hardware sensors [77]. Moreover, hardware sensors are not always available due to sensor maintenance or replacement, and soft sensors can be utilized as a backup [77]. In most chemical engineering applications, the process is time varying, multi-modal and nonlinear [77]. Therefore, it is necessary to improve

soft sensors to make them applicable for online prediction or model updates.

Many strategies have been applied to design soft sensor models. Ensemble learning is one of them. Kaneko and Funatsu developed Support Vector Regression (SVR) based adaptive soft sensor with Bayesian ensemble learning in [80]. In their work, predictions were first made with Online Support Vector Regression (OSVR), and these predictions were combined through Bayesian ensemble learning to obtain a final prediction. In the work by Kaneko and Funatsu [81], a final prediction is obtained by ensembling multiple predicted values from multiple intervals of time difference. Another adaptation mechanism for online prediction using soft sensors was proposed in [79]: Input variables selection is performed with mutual information. The selected variables are then used for prediction with a mixture of Gaussian Process Regression (GPR) models. Adaptation of combination weights and local GPR models are considered for a final prediction.

Besides ensemble learning, local learning frameworks have been used for soft sensor applications [82]. Kadlec and Gabrys proposed Incremental Local Learning Soft Sensing Algorithm (ILLSA) [82], where adaptations such as recursive adaptation of models and adaptation of combination weights could be performed. Also, another work by Kadlec and Gabrys [83] applies local learning to build online predictive models for the consideration of noise, drifting data and outliers. In this study, input space is partitioned to build several local models, and then predictions of different models are combined to obtain the final prediction.

We have introduced the design of soft sensors in terms of frameworks or strategies. The framework needs specific modelling approaches. Therefore, we also review soft sensor applications briefly from a modelling perspective. We have seen that Gaussian Process Regression has been used as soft sensors in [79]. Support Vector Regression (SVR) is another common choice for predictive modelling in chemical soft sensor applications. Bayesian approaches could ensemble SVR based models for a soft sensor development [80]. In [78], the author proposed a soft sensor framework, incorporating Bayesian Inference and SVR models to deal with measurement uncertainties, such as biases and misalignments. In this work, Bayesian Inference is applied first to process input measurements. The processed inputs are then used for two-stage SVR models. The second stage SVR serves as the main model to make predictions [78]. Besides

Gaussian Process Regression and Support Vector Regression, Partial Least Squares Regression is also a commonly used method in chemical process for soft sensing. Partial Least Squares Regression was applied for soft sensing in a refining process in petrochemical industry by Wang et al. [84], and in their work, PLS regression was enhanced to handle the dynamics of the process. Additionally, Shao and Tian built an adaptive soft sensor with local PLS models and Bayesian inference for model ensembles [85].

Based on the literature reviewed above, it can be deduced that there are multiple design approaches in soft sensing application, each of which have been proved to be useful. For example, the adaptiveness of soft sensors could use the advantages of different models, handle online outliers and uncertainties, as well as improve prediction accuracy. Also, most soft sensor designs focus on online applications. In this section, the studies of different soft sensor design approaches and algorithms are briefly introduced. In the next section, a novel idea will be introduced as the foundation for our proposed stacking soft sensor, which is based on stacking multiple predictive models.

4.2 A brief introduction to the idea of stacking models

The basics and preliminaries about stacking approaches are introduced in this section. A basic and general idea to combine multiple models called stacked generalization was proposed by Wolpert, and was designed to minimize the generalization error and reduce the bias of generalizers [86]. The core idea is to apply multiple levels of models to obtain a prediction. We give a stacking model with two levels for an example of this idea, as illustrated in Algorithm 1 below [86]. In particular, if there is one model in the first level, it becomes a model correction method [86].

Many combination strategies are available. Combining models linearly is one of the choices in the second level. For example, Breiman proposed a method to improve estimation performance by forming a linear combination of models. The coefficients of the combined model are constrained to be non-negative, and determined by cross-validation and least squares [87]. Also, for classification, the idea of stacking models

Algorithm 1 Procedures of stacking models of two levels

Step-1, inputs or features and outputs are applied to models in the first level to train separate models.

Step-2, the predictions of separate models from the first level, and the true values of outputs are applied to train a second level model.

Step-3, to predict a new input, it goes through two levels of models: separate predictions are made with models in the first level, then those predictions are used as inputs to make a prediction using the second level model.

Step-4, the prediction of the second level model is regarded as the final prediction.

with linear regression is studied in [88].

The model stacking approach has been studied for soft sensing. In [89], Napoli and Xibilia compared several model aggregation strategies for a Topping process in refinery plants, including applying PLS and Neural Network as an aggregation method in the second level. Additionally, in [90], the work focuses on stacking approaches in the Sulfur Recovery Unit, where the first level of models include Principal Component Analysis (PCA), Partial Least Squares (PLS) and Neural Networks (NN), and the second level can be simple average, Partial Least Squares (PLS) and Neural Networks (NN).

We learn from the above introduction that the idea of model stacking could be understood as a modelling ensemble framework, and it is flexible. In practice, when we implement the idea of stacking, there could be multiple levels, where each level could have multiple models and various types of models. Also, the models in the same level could have the same model structure or different model structures.

4.3 Revisit of Partial Least Squares Regression, Gaussian Process Regression and Support Vector Regression

In this section, three widely used algorithms in chemical engineering are introduced as offline soft sensor predictive models.

4.3.1 Partial Least Squares Regression

In this subsection, the main idea of Partial Least Squares Regression is introduced following the works of [91] and [92]. For more details on the algorithm and its implementation, the reader is referred to the original articles.

Partial Least Squares Regression (PLSR) has been widely used in chemometrics. It performs dimensionality reduction while making predictions. Distinct from Principal Component Analysis (PCA) which does decomposition only on input variables X , PLS aims to find components from input X , that are highly relevant to Y .

$$\begin{aligned} X &= TP^T + E \\ Y &= UQ^T + F \end{aligned} \tag{4.1}$$

where X and Y denote inputs and outputs, respectively. T is projections of X , and U is projections of Y . P and Q are loadings of X and Y , respectively. E and F denote error terms of X and Y , respectively. Covariance between T and U is maximized by decomposing X and Y .

A relationship between T and U could be obtained after the decomposition. The loadings of X and Y , the variable P and Q , are also determined after the decomposition. When we make predictions, we eliminate error terms by only considering the main components, or latent variables, P .

4.3.2 Gaussian Process Regression

In this subsection, we briefly review the Gaussian Process Regression [93] [94] [95].

Gaussian Process assumes that data could be regarded as a sample from a multivariate Gaussian distribution, and it is an extension of multivariate Gaussian distribution to infinite dimensions.

One characteristic of Gaussian Process is that it considers the distance between two points that are related by a covariance function, namely the kernel function. There are many types of covariance functions, Equation 4.2 shows the popularly used one, ‘‘Squared exponential’’:

$$k(x, x') = \sigma^2 e^{-\frac{(x-x')^2}{2l^2}} \tag{4.2}$$

where σ^2 denotes the maximum allowable covariance. x and x' are two data points.

It should be noted that Gaussian Process Regression produces a distribution of the variable to be predicted. The posterior distribution of a certain prediction y_* is :

$$y_*|y \sim \mathcal{N}(\mu_* + K_*^T K^{-1}(y - \mu), K_{**} - K_*^T K^{-1} K_*).$$

where μ and μ_* denote training means and test means. K denotes training set covariances, K_* denotes training-test set covariances, and K_{**} denotes test set covariances. The means could be set to 0 or be calculated by a selected mean function, and the covariances are calculated by the covariance function.

Maximum Likelihood Estimation is then applied to train the Gaussian Process Regression model. After training, the unknown parameters in the posterior distribution are obtained. It gives both a prediction value for the input and the uncertainty information. The mean value of the prediction distribution is considered to be the estimation value, while the variance of the prediction distribution provides the uncertainty information. Readers are referred to [93] [94] and [95] for more details.

4.3.3 Support Vector Regression

Support Vector Regression is the version of Support Vector Machine (SVM) for regression [34]. It utilizes the kernel based idea to deal with non-linearity. The normally used kernel functions are: linear function, polynomial function and radial basis function [36].

The core idea of feature expansion can be summarized as follows [35]: First, inputs are mapped non-linearly to a high dimensional space; then, a linear model is built in this new space. The solution of SVM is sparse, and only a subset of training data points are utilized to form the solution. Therefore, the subset of data points in training data which support the final solution are called support vectors.

Unlike the SVM used for classification, the Support Vector Regression applies an ϵ -insensitive loss function [34] [35]. Using this loss function, the optimization algorithm aims to minimize the error bound, rather than the observed training error [34] [35] [36]:

$$L_\epsilon(y, f(x)) = \begin{cases} 0 & \text{if } |y - f(x)| \leq \epsilon \\ |y - f(x)| & \text{otherwise} \end{cases}. \quad (4.3)$$

4.4 Design of stacking online soft sensor for SAGD process

The stacking online soft sensor for SAGD process including a description of its implementation is proposed in this section. The practicability and scalability are also demonstrated.

4.4.1 Design of the proposed soft sensor

We apply the idea of stacking models which was introduced in Section 4.2 to design the stacking online soft sensor in this section. Two levels of models are applied; the first level includes the offline predictive models and the second level includes the online correction model.

Normally, offline predictive models are selected as those tested to be useful in the targeted process. The number of offline predictive models is also flexible. Either one or multiple offline predictive models could be deployed. If multiple offline predictive models are implemented, we focus on the case where offline predictive models could compensate for each other. Also, the online model should be easy to implement, because it should not cause unbearable computational load. Thus, multiple linear regression is selected as the online update approach.

The workflow of schematic is described as:

1. Train offline predictive models using the historical dataset;
2. Learn weights and constant term of the online model by linear regression, with historical offline model predictions as inputs and historical measured output values as output;
3. A new data point to be predicted comes;
4. Make predictions for the new data point with offline predictive models, separately;
5. Offline predictions are combined linearly to form an updated online prediction.

The model combination weights and constant are learned in Step 2.

The schematic of the soft sensor online updated approach is shown in Figure 4.1.

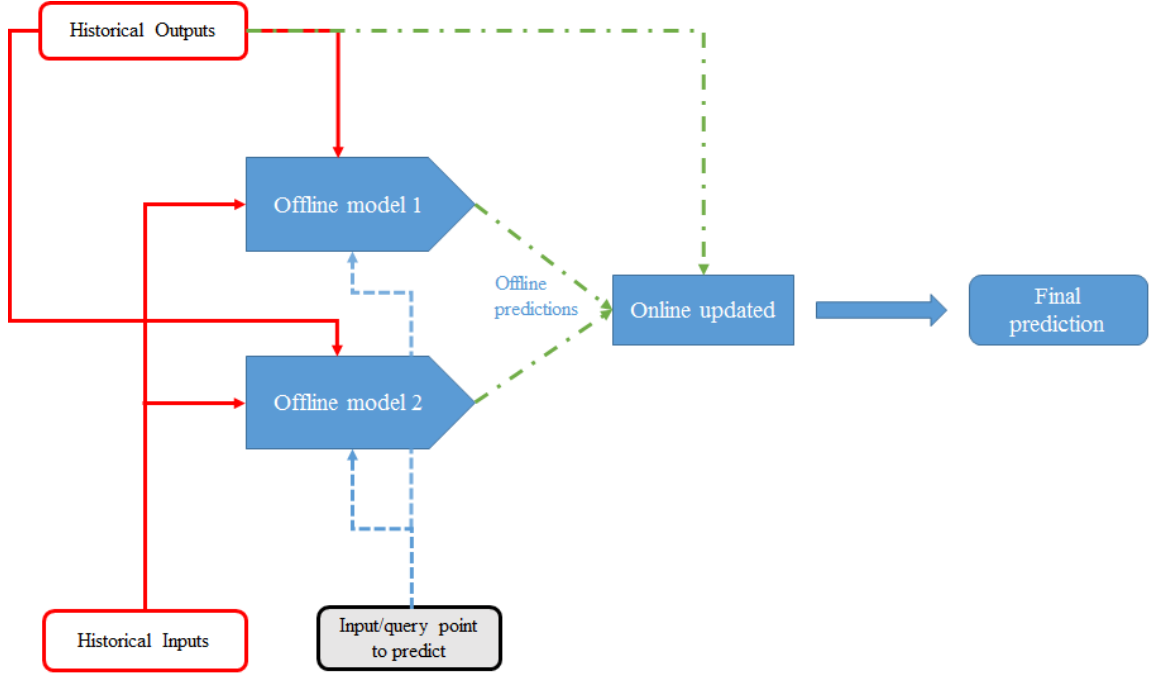


Figure 4.1: Schematic of smart online soft sensor

Now, we describe the model online update procedure in more details with two offline predictive models. This procedure can be extended to multiple offline models and shrunk to one offline model. We introduce the notations at the very beginning with descriptions of the implementation procedures.

Assume there are N data points in the historical dataset and each input sample contains p variables. $X_{N \times p}$ denotes historical inputs, and $Y_{N \times 1}$ denotes historical outputs. f_1 and f_2 denote two offline predictive models. O_1 and O_2 denote historical predictions from offline predictive models f_1 and f_2 , respectively.

The historical inputs in $X_{N \times p}$, are represented as:

$$\begin{bmatrix} x_{11} & x_{12} & x_{13} & \dots & x_{1p} \\ x_{21} & x_{22} & x_{23} & \dots & x_{2p} \\ \vdots & \vdots & \vdots & \ddots & \vdots \\ x_{N1} & x_{N2} & x_{N3} & \dots & x_{Np} \end{bmatrix}$$

The historical outputs in $Y_{N \times 1}$, are represented as:

$$\begin{bmatrix} y_1 \\ y_2 \\ \vdots \\ y_N \end{bmatrix}$$

Then, we train separate offline models on historical data, and obtain two separate offline models, $O_1 = f_1(X)$ and $O_2 = f_2(X)$. With those two offline models, we could also have offline predictions on historical data, say $O_{1N \times 1}$ and $O_{2N \times 1}$, which are regarded as a new dataset, denoted by matrix $O_{N \times 2}$:

$$\begin{bmatrix} o_{11} & o_{12} \\ o_{21} & o_{22} \\ \vdots & \vdots \\ o_{N1} & o_{N2} \end{bmatrix}$$

The online updates are based on the offline historical predictions $O_{N \times 2}$. Then, the online model update weights β_1 and β_2 , and constant term β_0 are learned by linear regression, with $O_{N \times 2}$ as inputs and $Y_{N \times 1}$ as outputs:

$$Y = \beta_0 + \beta_1 O_1 + \beta_2 O_2 \quad (4.4)$$

Thus far, the model of offline soft sensor and the online update models have been built. We now demonstrate how it make predictions. x_{new} denotes the new input to be predicted, which is of p dimensions. O_{1new} and O_{2new} denote predictions of x_{new} from the two offline predictive models. \hat{y}_{new} denotes the updated online prediction through stacking online soft sensor. There could potentially be two predictions for x_{new} from offline predictive models: $o_{1new} = f_1(x_{new})$ and $o_{2new} = f_2(x_{new})$.

Finally, update or correct the prediction with Equation 4.5 online as the final prediction for x_{new} :

$$\hat{y}_{new} = \beta_0 + \beta_1 o_{1new} + \beta_2 o_{2new} \quad (4.5)$$

where β_1 , β_2 and β_0 are coefficients of the linear regression model trained before, which is at the second level or online. This is a case of two offline predictive models. If there are more offline predictive models, coefficients should be extended accordingly and there is one constant term. For ease of implementation, we only deploy linear regression as the second level model, without adding non-negativity constraints. Since those offline predictions are independent of each other, the absolute value of coefficients such as β_1 and β_2 are interpreted as how much the corresponding offline prediction contributes to the final prediction. The signs of the coefficients, which could be positive, 0, or negative, and the constant term, play the role of combining the weighted offline predictions to adjust the bias of the prediction.

4.4.2 Practicability and scalability of the designed soft sensor

In this subsection, we show that the designed soft sensor approach is practicable and scalable from an implementation perspective.

Practicability

The weights and constant term are learned online by a simple linear model, which is easy to implement. We also observe that the proposed soft sensor does not rely on the model reconstruction of the offline predictive models, because the training of online simple model only uses offline historical predictions and historical outputs. Compared with complex or reconstructed models, this online update approach is fast, since the online model is simple. Moreover, the dimension of the dataset it needs to train the online model is equal to the number of offline models, which is expected to be less than the dimension of the inputs of offline models in practice. Therefore, there is no computation speed and storage issue, and hence, is practicable to implement.

Scalability

The number of offline models that can be used is flexible. If there are many offline models, each performs offline predictions separately. These independent predictions are then used as inputs in the online level to obtain a final prediction. When an offline model needs to be maintained or removed, the corresponding variable is removed in the online model, so it does not contribute to the final prediction. The online equation just needs to be retrained again with corresponding historical measurements and historical offline predictions. If one more offline model is added, only a column of data is added online as an additional feature for the online equation, and the online equation is updated by training a multiple linear regression model again. Note that the data for online equation are historical offline predictions and historical measurements. The number of historical offline predictions is equal to the number of offline predictive models, which is not large in practice. Thus, the dataset to train online equation is small. Also, the online equation is a multiple linear regression model, and hence, it is fast to retrain.

If there is only one offline model, it is the case of simple online model correction approach. The single offline prediction is corrected automatically via a linear regression

model, by using the information from its historical predictions and real measurements.

4.5 Application of stacking online soft sensor in SAGD process

This section demonstrates the usefulness of the proposed stacking online soft sensor, for two different applications in SAGD process.

In this regard, we apply multiple types of offline predictive models, which could compensate for each other. For the first level models or offline predictive models, we choose the pair of PLSR and GPR, as well as the pair of PLSR and SVR. Because PLSR can compensate for SVR and GPR, separately. PLSR could do dimensionality reduction, keeping the main information and explaining the linear relationship. GPR considers the similarity of inputs and the kernel explains the nonlinearity well. SVR does feature expansion with a kernel inside.

In order to evaluate the performance, prediction of the proposed soft sensor is compared with each offline prediction separately. In the applications under consideration, we show the results of testing data, or out-of-sample data. Statistical metrics such as Mean Absolute Error (MAE) and Mean Squared Error (MSE) of offline predictions and online updated predictions are calculated on testing data. Relative Improvement (RI) of these metrics are also evaluated to demonstrate the improvement of online predictions from offline predictions, which is defined as:

$$RI = (-1) * \frac{\text{metric of online prediction} - \text{metric of offline prediction}}{\text{metric of offline prediction}} * 100 \quad (4.6)$$

4.5.1 Case Study 1: Automatic Model Switching

We first demonstrate the application on a dataset of a simulated SAGD process. In this case, we show that online update approach designed here plays a role of automatic online switching of offline predictive models, while simultaneously keeping the good offline model predictions.

We make predictions of Annulus Reservoir Pressure. Offline soft sensor models are Gaussian Process (GP) and Partial Least Squares Regression (PLSR). Gaussian

Process is chosen since it is a Bayesian modelling approach as well as a correlation-based model, which is useful in solving the regression problem. Partial Least Squares Regression (PLSR) is chosen for its ability to perform dimensionality reduction, and also for its potential usefulness in soft sensor applications. These models work in different perspectives and could compensate for each other. As described before, online update approach is multiple linear regression.

We show three separate testing cases on this simulated dataset. Since it is a soft sensor application, training and testing datasets are divided chronologically. The training and testing periods along with timeline are shown in Figure 4.2. In the first period, we have 200 training samples and 200 testing samples. In the second and third period, we have 450 training samples and 240 testing samples, as well as 550 training samples and 240 testing samples, respectively. In different training periods, the offline predictive models are retrained with the available training data in that period. The retrained offline predictions are tested with testing data of that period. The online linear model coefficients are also retrained with offline predictions and historical outputs in that training period. The online predictions are tested using testing data in that period.

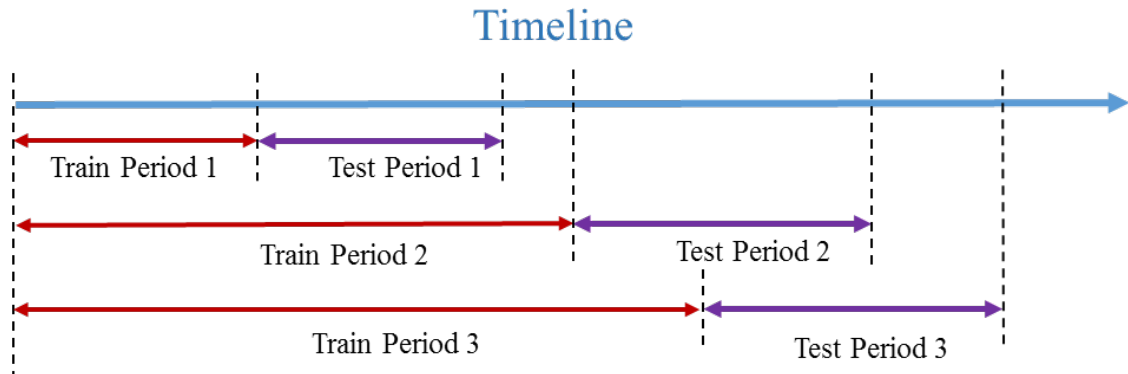


Figure 4.2: Training and testing data partition along with timeline

The description of inputs or features and outputs of simulated dataset is shown in Table 4.1.

Table 4.1: Description of variables of simulated dataset

	Variable Name	Units
Output	Annulus Reservoir Pressure	psia
Feature 1	Injection Tubing Pressure	psia
Feature 2	Injection Tubing Temperature	deg F
Feature 3	Water Injected Flowrate	STB/day
Feature 4	Liquid Produced Flowrate	STB/day

The testing results of three chronologically partitioned periods, which are shown in Figure 4.2, are demonstrated below. In each period, the results are demonstrated in terms of online equation which is learned from training data, as well as prediction plots and statistical metrics on testing data.

Period1

First, we present the model update equation learned online using training data (historical offline predictions and historical measured values):

$$\begin{aligned}
 \hat{y} \text{ (online prediction)} &= 0.99925 \times O_1 \text{ (PLSR offline prediction)} \\
 &+ 0.00148 \times O_2 \text{ (GP offline prediction)} \\
 &- 0.15738 \text{ (constant term)}
 \end{aligned} \tag{4.7}$$

Equation 4.7 shows that the PLSR model has larger weight than GPR model. PLSR almost dominates the updated prediction in this period.

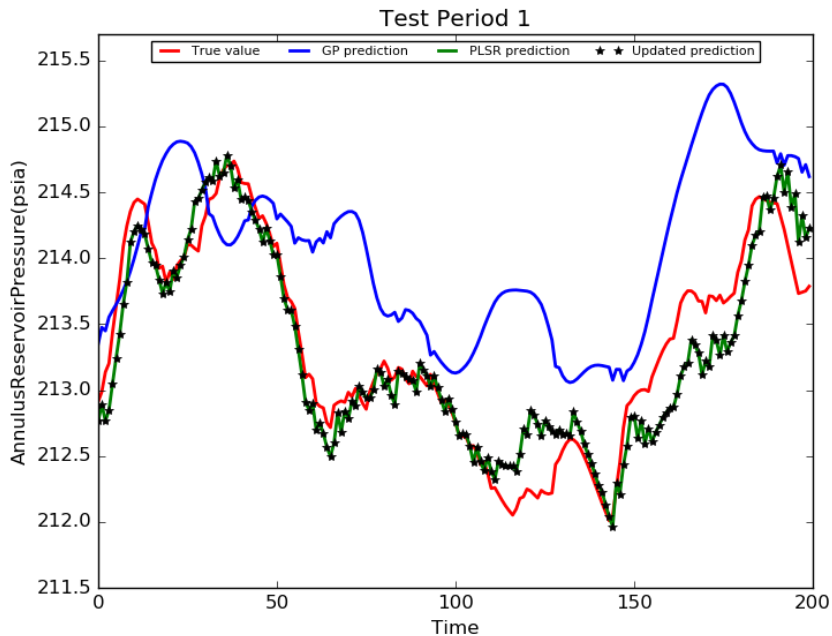


Figure 4.3: Performance on test data in Period 1

Figure 4.3 shows the test results in Period 1. We see that PLSR follows the trend of true value very well while GP performs worse than PLSR in this period. The updated prediction is very close to the PLSR prediction since PLSR has larger weight and dominates the final prediction. Therefore, in this period, the online prediction “switches” to offline PLSR model.

The statistical metrics on testing data are presented in Table 4.2. The Relative Improvement (RI) from GPR is a large value, but the RI from PLSR is very small. Because GPR has not performed well and PLSR has performed well in this period. These RIs indicate that the online prediction or the automatic “switch” does not lose performance; instead, there is even slight improvement in this period.

Table 4.2: Statistical metrics on test data in Period 1

	Test MAE	Test MSE
Offline GP	0.76722	0.79187
Offline PLSR	0.21454	0.07429
Online Prediction	0.21411	0.07405
RI from GP	72.092%	90.648%
RI from PLSR	0.200%	0.323%

Period2

We continue to Period 2. We train and predict the model with the same hyperparameter settings as Period 1. We first show the learned online model update equation using training data, written as Equation 4.8:

$$\begin{aligned} \hat{y} \text{ (online prediction)} &= -0.09116 \times O_1 \text{ (PLSR offline prediction)} \\ &+ 1.15640 \times O_2 \text{ (GP offline prediction)} \\ &- 13.91435 \text{ (constant term)} \end{aligned} \quad (4.8)$$

From the above equation, we see that in this period, GPR dominates the final prediction and it has larger absolute value of weight than that of PLSR. It is different from the case in Period 1, where PLSR dominates the final prediction.

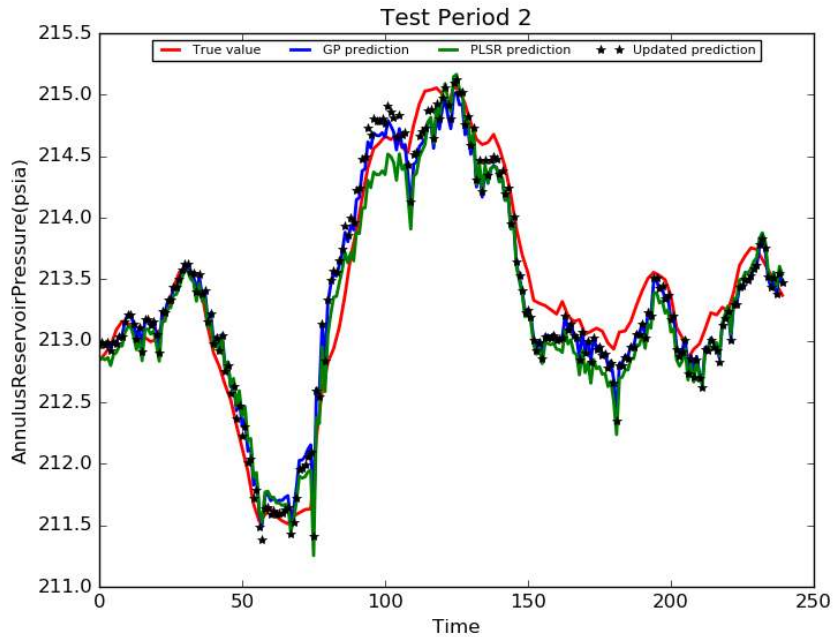


Figure 4.4: Performance on test data in Period 2

From Figure 4.4, it can be observed that the updated predictions are very close to GPR predictions, and they are dominated by GPR, because most of the black stars almost lie on the blue line.

GPR predictions are closer to true values than PLSR predictions. The blue line is closer to the red line than the green line. It can also be observed from the statistical metrics presented in Table 4.3.

Table 4.3: Statistical metrics on test data in Period 2

	Test MAE	Test MSE
Offline GP	0.18804	0.05307
Offline PLSR	0.20923	0.06259
Online Prediction	0.18274	0.05106
RI from GP	2.818%	3.787%
RI from PLSR	12.660%	18.421%

From Table 4.3, it can be seen that GPR performs better than PLSR in this period, and the online predictions have improvements from both offline predictive models. Recall that in the first period, PLSR dominates the final prediction, however, GPR dominates in the second period. We do not need to determine the dominated model manually, and the online update approach could choose the dominated one or “switch” automatically.

Period3

We follow the procedure as followed in previous periods. In Period 3, offline models keep their previous hyperparameter settings, without retuning hyperparameters. Firstly, the online model update equation is shown in Equation 4.9:

$$\begin{aligned} \hat{y} \text{ (online prediction)} = & -0.08315 \times O_1 \text{ (PLSR offline prediction)} \\ & + 1.14005 \times O_2 \text{ (GP offline prediction)} \\ & - 12.13169 \text{ (constan term)} \end{aligned} \quad (4.9)$$

We learn from Equation 4.9 that in this period, GPR also dominates the final prediction, and PLSR contributes much less, since the former has larger absolute value of weight. This equation is learned from training data. The conclusion that GPR dominates the online prediction, should also be validated in test data. Figure 4.5 shows the prediction plot of two offline models and the online update prediction on test data of Period 3.

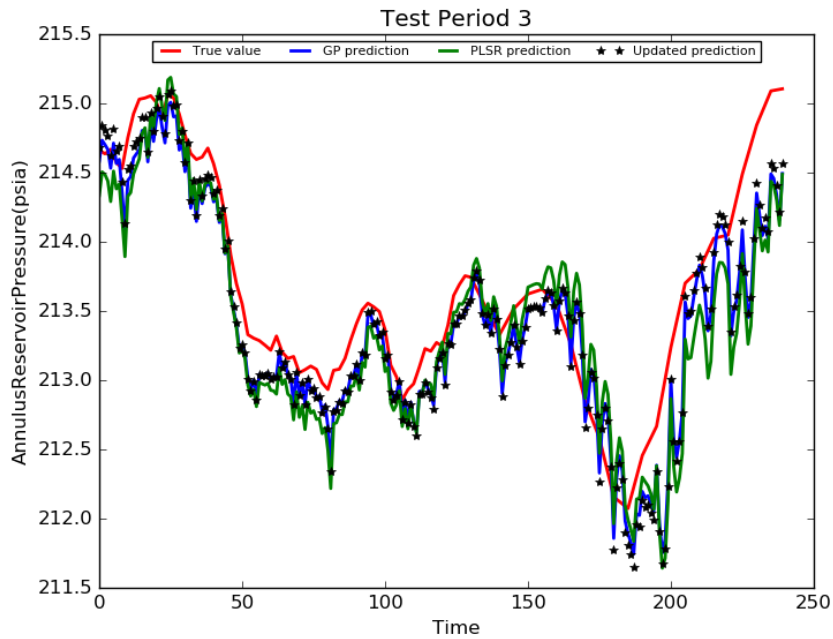


Figure 4.5: Performance on test data in Period 3

In Figure 4.5, black stars almost lie on the blue line, meaning that online updated predictions are closer to GPR offline predictions than PLSR offline predictions. Also, the figure illustrates that GPR offline predictions perform better than PLSR offline predictions. Because the blue line is closer to the red line than the green line overall. Now, let us see the statistical metrics in Table 4.4.

Table 4.4: Statistical metrics on test data in Period 3

	Test MAE	Test MSE
Offline GP	0.28263	0.13567
Offline PLSR	0.34561	0.19946
Online Prediction	0.27494	0.13095
RI from GP	2.720%	3.479%
RI from PLSR	20.447%	34.347%

In Period 3, it has similar performance to that of Period 2. GPR performs better and the online approach keeps this from Period 2 to Period 3, without switching models. Moreover, it makes slight improvements simultaneously while keeping the dominated model.

So, in this study case, from the above analysis of the 3 testing results, we show that the online model updated approach not only plays the role of an automatic offline model “switch”, but also makes improvements from any offline predictive model. The online model equation is changing when dataset are updated, and it is learned online automatically.

4.5.2 Case Study 2: Model Performance Improvement

In this case study, we validate the online model update approach via an industrial dataset. This study case emphasizes that the online predictions are improved significantly from offline predictions. Training dataset contains 2,000 data points and testing dataset contains 800 data points. Both of them have 18 features coming from a well-pair for the development of water content soft sensor in SAGD process. The output variable is water content. For data proprietary, the name and units of features for predicting output are not listed, and also, only normalized results are reported in the plot and statistical metrics.

PLSR and SVR are selected as offline soft sensor models based on experience. PLSR is selected for dimensionality reduction, and SVR is selected for its idea of feature expansion. Those two models compensate for each other according to their model characteristics. A compensation of them is expected online.

Online model update equation learned on industrial training dataset:

$$\begin{aligned} \hat{y} \text{ (online prediction)} &= 0.35191 \times O_1 \text{ (PLSR offline prediction)} \\ &+ 1.10563 \times O_2 \text{ (SVR offline prediction)} \quad (4.10) \\ &- 0.21650 \text{ (constant term)} \end{aligned}$$

Online model update equation learned from training data is presented in Equation 4.10. We observe that though SVR dominates the prediction, PLSR still contributes noticeably. Table 4.5 shows the statistical metrics on test data. We see that in view of MAE, PLSR performs slightly better than SVR, whereas in view of MSE, SVR performs better than PLSR. This occurs for the reason that MSE performs the calculation of square of the error before averaging whereas MAE only does an absolute value calculation, and therefore MSE penalizes more about larger errors. SVR not only performs feature expansion, but also performs an ϵ -regression, which

was introduced in subsection 4.3.3.

Table 4.5: Statistical metrics on industrial test data

	Test MAE	Test MSE
Offline SVR	0.38704	0.20691
Offline PLSR	0.36722	0.37824
Online Prediction	0.27587	0.15479
RI from SVR	28.723%	25.189%
RI from PLSR	24.876%	59.076%

We learn from RIs in Table 4.5, that the predictions of online updated approach perform better than either of the offline model considerably. Also, this is demonstrated by Figure 4.6.

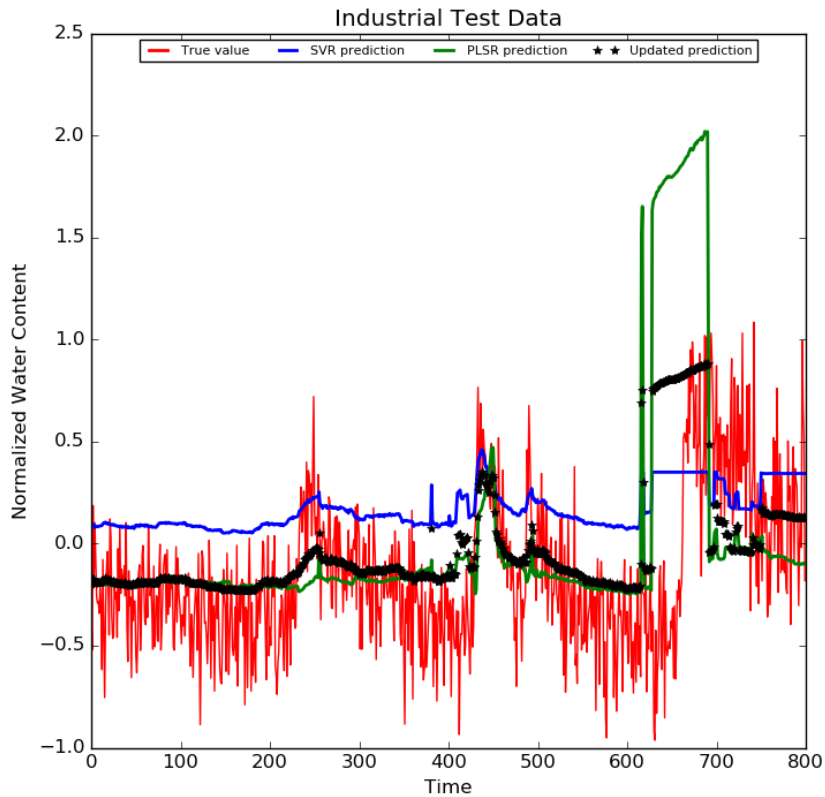


Figure 4.6: Performance on industrial test data

This case study shows that the model online approach could ensemble offline models and make better predictions than either offline model, since the two offline models

could compensate for each other in their model characteristics.

4.6 Conclusions

In this chapter, the stacking online soft sensor in SAGD process is proposed, for the purpose of correcting the offline model predictions. This soft sensor applies the idea of stacking models, conducting a two-level hierarchy of models. The first level contains offline predictive models, and the second level provides online update or corrections using a linear regression model. Also, the practicability and scalability of the proposed soft sensor are discussed. The online update approach is chosen as linear regression because it is a simple model and easy to implement. Then, two case studies are presented to validate the effectiveness of the proposed soft sensor in SAGD process. The first case study shows that this stacking online soft sensor could play the role of an automatic online switch, while keeping the offline prediction performance. The second case study shows that the proposed soft sensor could make use of the advantages of different models and improve the performance of the combined models.

Chapter 5

Conclusions

5.1 Summary of This Thesis

This thesis focuses on data mining and optimization in SAGD process. Chapter 1 included motivation, contributions and outline of this thesis.

Machine learning is a popular topic recently, and has wide applications in Image Processing and Natural Language Processing. In Chapter 2, a comparative study of multiple popularly used machine learning algorithms are performed in oil sands subcool monitoring. Regression models were built, with subcool as the predictive variable, and injection casing pressure, injection tubing pressure, injection casing flowrate, injection tubing flowrate and pump frequency as input variables. The widely used machine learning algorithms with good practical merit compared in this study case were Deep Learning, Gradient Boosted Decision Trees, Random Forest, Support Vector Regression, as well as Ridge Regression and Multiple Linear Regression. This chapter discussed advantages of these algorithms by analyzing the results. Also, investigation of original data with a different set of results showed that priori knowledge and data quality should be taken into consideration while using machine learning to perform data analytics in oil sands problems.

Chapter 3 proposed a method called Locally Weighted Quadratic Regression based Bayesian Optimization (LWQRBO). This method inherits the framework of Bayesian Optimization with Expected Improvement. Locally weighted quadratic regression was applied to build the surrogate model. Genetic Algorithm (GA) was applied as a subsolver to maximize Expected Improvement for determining the next sample point within the optimization algorithm. Two numerical case studies were applied to test

its performance. Further, the proposed LWQRBO was applied to solve the SAGD optimization problem.

Soft sensors play an important role in SAGD process, especially when hardware sensors are not available. Chapter 4 presented the design of a stacking online soft sensor. It was inspired by the idea of stacking models, so it is called stacking online soft sensor. This design consists of two levels of models. Models which could compensate for each other were deployed as the first level models. Multiple linear regression was deployed as the second level model, since it is simple and easy to implement. Two case studies, Annul Reservoir Pressure soft sensor application and Water Content soft sensor application, were presented to validate its usefulness in SAGD process.

5.2 Directions for Future Work

Future work can be extended in two directions, Bayesian Optimization in SAGD process and Ensemble models for soft sensor.

1. Though the framework of Bayesian Optimization has been well established, many components could be modified, especially the surrogate model and the figure of merit to sample the next iteration point. They could be adjusted accordingly since the choice of model and the figure of merit depend on the problem or the process that we are interested in. The work of [51] can be used as a guide for adjustments of components in the existing framework.

2. Inspired by the sampling strategy in Bayesian Optimization, the idea of Bayesian can be considered to be embedded into the MPC framework, by adding a Bayesian component into existing MPC, or be embedded into the adaptive optimal control framework. More research and literature review should be done on this.

3. Model error correction methods or cascade modelling approaches can be considered for the improvement of soft sensor approaches. Bayesian model ensemble method is also a choice to improve soft sensor performance.

4. The ensemble of feature extraction (slow features or fast features) and stacking model is a promising direction. Different models could be used to process different types of features or extracted features.

Bibliography

- [1] Roger Butler et al. Sagd comes of age! *Journal of Canadian Petroleum Technology*, 37(07), 1998.
- [2] As Muatasim Mohammad Al Bahlani, Tayfun Babadagli, et al. A critical review of the status of sagd: Where are we and what is next? In *SPE western regional and Pacific section AAPG joint meeting*. Society of Petroleum Engineers, 2008.
- [3] T Chung, W Bae, J Lee, W Lee, and B Jung. A review of practical experience and management of the sagd process for oil sands development. *Energy Sources, Part A: Recovery, Utilization, and Environmental Effects*, 34(3):219–226, 2011.
- [4] Shahab D Mohaghegh, Abi Modavi, Hafez Hafez, Masoud Haajizadeh, and Srikant Guruswamy. Development of surrogate reservoir model (srm) for fast track analysis of a complex reservoir. *International Journal of Oil, Gas and Coal Technology*, 2(1):2–23, 2009.
- [5] Colin C Card, Neilin Chakrabarty, Ian D Gates, et al. Automated global optimization of commercial sagd operations. In *Canadian International Petroleum Conference*. Petroleum Society of Canada, 2006.
- [6] PA Vander Valk, P Yang, et al. Investigation of key parameters in sagd wellbore design and operation. *Journal of Canadian Petroleum Technology*, 46(06):49–56, 2007.
- [7] Jian-Yang Yuan, Daniel Nugent, et al. Subcool, fluid productivity, and liquid level above a sagd producer. *Journal of Canadian Petroleum Technology*, 52(05): 360–367, 2013.

- [8] Dharmeshkumar R Gotawala, Ian D Gates, et al. A basis for automated control of steam trap subcool in sagd. *SPE Journal*, 17(03):680–686, 2012.
- [9] Y Ito, S Suzuki, et al. Numerical simulation of the sagd process in the hangingstone oil sands reservoir. *Journal of Canadian Petroleum Technology*, 38(09), 1999.
- [10] KE Kisman et al. Artificial lift, a major unresolved issue for sagd. In *Canadian International Petroleum Conference*. Petroleum Society of Canada, 2001.
- [11] Dharmesh Rameshchandra Gotawala, Ian Donald Gates, et al. Sagd subcool control with smart injection wells. In *EUROPEC/EAGE Conference and Exhibition*. Society of Petroleum Engineers, 2009.
- [12] TW Stone and WJ Bailey. Optimization of subcool in sagd bitumen processes. In *Prepared for presentation at the 2014 World Heavy Oil Congress, New Orleans*, pages 5–7, 2014.
- [13] Kalpesh Patel, Elvira M Aske, Morten Fredriksen, et al. Use of model-predictive control for automating sagd well-pair operations: A simulation study. *SPE Production & Operations*, 29(02):105–113, 2014.
- [14] Elvira Marie Aske, Morten Fredriksen, Kalpesh Patel, et al. Integrating reservoir simulator and model predictive control software for automating sagd well pair operations. In *SPE Heavy Oil Conference-Canada*. Society of Petroleum Engineers, 2013.
- [15] Ian Goodfellow, Yoshua Bengio, and Aaron Courville. *Deep learning*. MIT press, 2016.
- [16] Yann LeCun, Yoshua Bengio, and Geoffrey Hinton. Deep learning. *Nature*, 521(7553):436–444, 2015.
- [17] Ian Goodfellow, Jean Pouget-Abadie, Mehdi Mirza, Bing Xu, David Warde-Farley, Sherjil Ozair, Aaron Courville, and Yoshua Bengio. Generative adversarial nets. In *Advances in neural information processing systems*, pages 2672–2680, 2014.

- [18] Kurt Hornik, Maxwell Stinchcombe, and Halbert White. Multilayer feedforward networks are universal approximators. *Neural networks*, 2(5):359–366, 1989.
- [19] Andrew M Saxe, James L McClelland, and Surya Ganguli. Exact solutions to the nonlinear dynamics of learning in deep linear neural networks. *arXiv preprint arXiv:1312.6120*, 2013.
- [20] Léon Bottou. Stochastic gradient descent tricks. In *Neural networks: Tricks of the trade*, pages 421–436. Springer, 2012.
- [21] Xavier Glorot and Yoshua Bengio. Understanding the difficulty of training deep feedforward neural networks. In *Proceedings of the Thirteenth International Conference on Artificial Intelligence and Statistics*, pages 249–256, 2010.
- [22] Vinod Nair and Geoffrey E Hinton. Rectified linear units improve restricted boltzmann machines. In *Proceedings of the 27th international conference on machine learning (ICML-10)*, pages 807–814, 2010.
- [23] Andrew L Maas, Awni Y Hannun, and Andrew Y Ng. Rectifier nonlinearities improve neural network acoustic models. In *Proc. ICML*, volume 30, 2013.
- [24] Djork-Arné Clevert, Thomas Unterthiner, and Sepp Hochreiter. Fast and accurate deep network learning by exponential linear units (elus). *arXiv preprint arXiv:1511.07289*, 2015.
- [25] Léon Bottou. Large-scale machine learning with stochastic gradient descent. In *Proceedings of COMPSTAT’2010*, pages 177–186. Springer, 2010.
- [26] John Duchi, Elad Hazan, and Yoram Singer. Adaptive subgradient methods for online learning and stochastic optimization. *Journal of Machine Learning Research*, 12(Jul):2121–2159, 2011.
- [27] Diederik Kingma and Jimmy Ba. Adam: A method for stochastic optimization. *arXiv preprint arXiv:1412.6980*, 2014.
- [28] Jerome H Friedman. Greedy function approximation: a gradient boosting machine. *Annals of statistics*, pages 1189–1232, 2001.

- [29] Jerome H Friedman. Stochastic gradient boosting. *Computational Statistics & Data Analysis*, 38(4):367–378, 2002.
- [30] Jerome Friedman, Trevor Hastie, and Robert Tibshirani. *The elements of statistical learning*, volume 1. Springer series in statistics New York, 2001.
- [31] Yoav Freund, Robert Schapire, and Naoki Abe. A short introduction to boosting. *Journal-Japanese Society For Artificial Intelligence*, 14(771-780):1612, 1999.
- [32] Leo Breiman. Random forests. *Machine learning*, 45(1):5–32, 2001.
- [33] Miao Liu, Mingjun Wang, Jun Wang, and Duo Li. Comparison of random forest, support vector machine and back propagation neural network for electronic tongue data classification: Application to the recognition of orange beverage and chinese vinegar. *Sensors and Actuators B: Chemical*, 177:970–980, 2013.
- [34] Corinna Cortes and Vladimir Vapnik. Support-vector networks. *Machine learning*, 20(3):273–297, 1995.
- [35] Debasish Basak, Srimanta Pal, and Dipak Chandra Patranabis. Support vector regression. *Neural Information Processing-Letters and Reviews*, 11(10):203–224, 2007.
- [36] Alex J Smola and Bernhard Schölkopf. A tutorial on support vector regression. *Statistics and computing*, 14(3):199–222, 2004.
- [37] Yoshua Bengio et al. Learning deep architectures for ai. *Foundations and trends[®] in Machine Learning*, 2(1):1–127, 2009.
- [38] Nitish Srivastava, Geoffrey E Hinton, Alex Krizhevsky, Ilya Sutskever, and Ruslan Salakhutdinov. Dropout: a simple way to prevent neural networks from overfitting. *Journal of machine learning research*, 15(1):1929–1958, 2014.
- [39] François Chollet et al. Keras. <https://github.com/fchollet/keras>, 2015.
- [40] Martín Abadi, Ashish Agarwal, Paul Barham, Eugene Brevdo, Zhifeng Chen, Craig Citro, Greg S. Corrado, Andy Davis, Jeffrey Dean, Matthieu Devin, Sanjay Ghemawat, Ian Goodfellow, Andrew Harp, Geoffrey Irving, Michael Isard,

- Yangqing Jia, Rafal Jozefowicz, Lukasz Kaiser, Manjunath Kudlur, Josh Levenberg, Dan Mané, Rajat Monga, Sherry Moore, Derek Murray, Chris Olah, Mike Schuster, Jonathon Shlens, Benoit Steiner, Ilya Sutskever, Kunal Talwar, Paul Tucker, Vincent Vanhoucke, Vijay Vasudevan, Fernanda Viégas, Oriol Vinyals, Pete Warden, Martin Wattenberg, Martin Wicke, Yuan Yu, and Xiaoqiang Zheng. TensorFlow: Large-scale machine learning on heterogeneous systems, 2015. URL <https://www.tensorflow.org/>. Software available from tensorflow.org.
- [41] Fabian Pedregosa, Gaël Varoquaux, Alexandre Gramfort, Vincent Michel, Bertrand Thirion, Olivier Grisel, Mathieu Blondel, Peter Prettenhofer, Ron Weiss, Vincent Dubourg, et al. Scikit-learn: Machine learning in python. *Journal of Machine Learning Research*, 12(Oct):2825–2830, 2011.
- [42] Lars Buitinck, Gilles Louppe, Mathieu Blondel, Fabian Pedregosa, Andreas Mueller, Olivier Grisel, Vlad Niculae, Peter Prettenhofer, Alexandre Gramfort, Jaques Grobler, et al. Api design for machine learning software: experiences from the scikit-learn project. *arXiv preprint arXiv:1309.0238*, 2013.
- [43] Luis Miguel Rios and Nikolaos V Sahinidis. Derivative-free optimization: a review of algorithms and comparison of software implementations. *Journal of Global Optimization*, 56(3):1247–1293, 2013.
- [44] Charles Audet and John E Dennis Jr. Mesh adaptive direct search algorithms for constrained optimization. *SIAM Journal on optimization*, 17(1):188–217, 2006.
- [45] Donald R Jones, Matthias Schonlau, and William J Welch. Efficient global optimization of expensive black-box functions. *Journal of Global optimization*, 13(4):455–492, 1998.
- [46] Robert B Gramacy, Genetha A Gray, Sébastien Le Digabel, Herbert KH Lee, Pritam Ranjan, Garth Wells, and Stefan M Wild. Modeling an augmented lagrangian for blackbox constrained optimization. *Technometrics*, 58(1):1–11, 2016.

- [47] Victor Picheny, Robert B Gramacy, Stefan Wild, and Sebastien Le Digabel. Bayesian optimization under mixed constraints with a slack-variable augmented lagrangian. In *Advances in Neural Information Processing Systems*, pages 1435–1443, 2016.
- [48] Jack PC Kleijnen, Wim van Beers, and Inneke Van Nieuwenhuysse. Expected improvement in efficient global optimization through bootstrapped kriging. *Journal of global optimization*, pages 1–15, 2012.
- [49] Felipe AC Viana, Raphael T Haftka, and Layne T Watson. Efficient global optimization algorithm assisted by multiple surrogate techniques. *Journal of Global Optimization*, 56(2):669–689, 2013.
- [50] Jasper Snoek, Hugo Larochelle, and Ryan P Adams. Practical bayesian optimization of machine learning algorithms. In *Advances in neural information processing systems*, pages 2951–2959, 2012.
- [51] Ky Khac Vu, Claudia D’Ambrosio, Youssef Hamadi, and Leo Liberti. Surrogate-based methods for black-box optimization. *International Transactions in Operational Research*, 24(3):393–424, 2017.
- [52] Philipp Hennig and Christian J Schuler. Entropy search for information-efficient global optimization. *Journal of Machine Learning Research*, 13(Jun):1809–1837, 2012.
- [53] Bastien Talgorn, Charles Audet, Sébastien Le Digabel, and Michael Kokkolaras. Locally weighted regression models for surrogate-assisted design optimization.
- [54] Andrew R Conn and Sébastien Le Digabel. Use of quadratic models with mesh-adaptive direct search for constrained black box optimization. *Optimization Methods and Software*, 28(1):139–158, 2013.
- [55] Cong Kein Dang. *Optimization of algorithms with the OPAL framework*. PhD thesis, École Polytechnique de Montréal, 2012.
- [56] Zhong-Hua Han and Ke-Shi Zhang. Surrogate-based optimization. In *Real-World Applications of Genetic Algorithms*. InTech, 2012.

- [57] Slawomir Koziel and Leifur Leifsson. Surrogate-based modeling and optimization. *Applications in Engineering*, 2013.
- [58] Yolanda Mack, Tushar Goel, Wei Shyy, and Raphael Haftka. Surrogate model-based optimization framework: a case study in aerospace design. *Evolutionary computation in dynamic and uncertain environments*, pages 323–342, 2007.
- [59] Xiaofeng Yuan, Biao Huang, Zhiqiang Ge, and Zhihuan Song. Double locally weighted principal component regression for soft sensor with sample selection under supervised latent structure. *Chemometrics and Intelligent Laboratory Systems*, 153:116–125, 2016.
- [60] Zhiqiang Ge and Zhihuan Song. A comparative study of just-in-time-learning based methods for online soft sensor modeling. *Chemometrics and Intelligent Laboratory Systems*, 104(2):306–317, 2010.
- [61] Xiaofeng Yuan, Zhiqiang Ge, Biao Huang, and Zhihuan Song. A probabilistic just-in-time learning framework for soft sensor development with missing data. *IEEE Transactions on Control Systems Technology*, 25(3):1124–1132, 2017.
- [62] Xiaofeng Yuan, Zhiqiang Ge, Biao Huang, Zhihuan Song, and Yalin Wang. Semisupervised jitl framework for nonlinear industrial soft sensing based on locally semisupervised weighted pcr. *IEEE Transactions on Industrial Informatics*, 13(2):532–541, 2017.
- [63] Christopher G. Atkeson, Andrew W. Moore, and Stefan Schaal. Locally weighted learning. *Artificial Intelligence Review*, 11(1):11–73, Feb 1997. ISSN 1573-7462. doi: 10.1023/A:1006559212014. URL <https://doi.org/10.1023/A:1006559212014>.
- [64] S. Surjanovic and D. Bingham. Virtual library of simulation experiments: Test functions and datasets. Retrieved November 20, 2017, from <http://www.sfu.ca/~ssurjano>.
- [65] Giancarlo Giacchetta, Mariella Leporini, and Barbara Marchetti. Economic and

- environmental analysis of a steam assisted gravity drainage (sagd) facility for oil recovery from canadian oil sands. *Applied Energy*, 142:1–9, 2015.
- [66] Mahyar Matt Mohajer, Carlos Emilio Perez Damas, Alexander Jose Berbin Silva, Andreas Al-Kinani, et al. An integrated framework for sagd real-time optimization. In *SPE Intelligent Energy Conference and Exhibition*. Society of Petroleum Engineers, 2010.
- [67] H Shin, M Polikar, et al. Review of reservoir parameters to optimize sagd and fast-sagd operating conditions. *Journal of Canadian Petroleum Technology*, 46(01), 2007.
- [68] S Thomas. Enhanced oil recovery-an overview. *Oil & Gas Science and Technology-Revue de l'IFP*, 63(1):9–19, 2008.
- [69] Neil Edmunds, Simon D Gittins, et al. Effective application of steam assisted gravity drainage of bitumen to long horizontal well pairs. *Journal of Canadian Petroleum Technology*, 32(06):49–55, 1993.
- [70] ID Gates, N Chakrabarty, et al. Optimization of steam-assisted gravity drainage in mcmurray reservoir. In *Canadian International Petroleum Conference*. Petroleum Society of Canada, 2005.
- [71] Card Yang, C Card, L Nghiem, et al. Economic optimization and uncertainty assessment of commercial sagd operations. In *Canadian International Petroleum Conference*. Petroleum Society of Canada, 2007.
- [72] John David Michael Belgrave, Ben Ifeanyi Nzekwu, Harbir S Chhina, et al. Sagd optimization with air injection. In *Latin American & Caribbean Petroleum Engineering Conference*. Society of Petroleum Engineers, 2007.
- [73] Chaodong Yang, Colin Card, Long X Nghiem, Eugene Fedutenko, et al. Robust optimization of sagd operations under geological uncertainties. In *SPE Reservoir Simulation Symposium*. Society of Petroleum Engineers, 2011.

- [74] Shahed Rahim and Zukui Li. Reservoir geological uncertainty reduction: an optimization-based method using multiple static measures. *Mathematical Geosciences*, 47(4):373–396, 2015.
- [75] Eugene Fedutenko, Chaodong Yang, Colin Card, and Long Nghiem. Optimization of sagd process accounting for geological uncertainties using proxy models. *Proceedings of CSPG/CSEG/CWLS GeoConvention.(6-12 May), Calgary, AB, Canada*, 2013.
- [76] Nestor V Queipo, Javier V Goicochea, and Salvador Pintos. Surrogate modeling-based optimization of sagd processes. *Journal of Petroleum Science and Engineering*, 35(1):83–93, 2002.
- [77] Dražen Slišković, Ratko Grbić, and Željko Hocenski. Methods for plant data-based process modeling in soft-sensor development. *Automatika*, 52(4):306–318, 2011.
- [78] Jie Yu. A bayesian inference based two-stage support vector regression framework for soft sensor development in batch bioprocesses. *Computers & Chemical Engineering*, 41:134–144, 2012.
- [79] Ratko Grbić, Dražen Slišković, and Petr Kadlec. Adaptive soft sensor for online prediction and process monitoring based on a mixture of gaussian process models. *Computers & chemical engineering*, 58:84–97, 2013.
- [80] Hiromasa Kaneko and Kimito Funatsu. Adaptive soft sensor based on online support vector regression and bayesian ensemble learning for various states in chemical plants. *Chemometrics and Intelligent Laboratory Systems*, 137:57–66, 2014.
- [81] Hiromasa Kaneko and Kimito Funatsu. A soft sensor method based on values predicted from multiple intervals of time difference for improvement and estimation of prediction accuracy. *Chemometrics and Intelligent Laboratory Systems*, 109(2):197–206, 2011.

- [82] Petr Kadlec and Bogdan Gabrys. Local learning-based adaptive soft sensor for catalyst activation prediction. *AIChE Journal*, 57(5):1288–1301, 2011.
- [83] Petr Kadlec and Bogdan Gabrys. Soft sensor based on adaptive local learning. In *International Conference on Neural Information Processing*, pages 1172–1179. Springer, 2008.
- [84] David Wang, Jun Liu, and Rajagopalan Srinivasan. Data-driven soft sensor approach for quality prediction in a refining process. *IEEE Transactions on Industrial Informatics*, 6(1):11–17, 2010.
- [85] Weiming Shao and Xuemin Tian. Adaptive soft sensor for quality prediction of chemical processes based on selective ensemble of local partial least squares models. *Chemical Engineering Research and Design*, 95:113–132, 2015.
- [86] David H Wolpert. Stacked generalization. *Neural networks*, 5(2):241–259, 1992.
- [87] Leo Breiman. Stacked regressions. *Machine learning*, 24(1):49–64, 1996.
- [88] Saso Džeroski and Bernard Ženko. Is combining classifiers with stacking better than selecting the best one? *Machine learning*, 54(3):255–273, 2004.
- [89] Giuseppe Napoli and Maria Gabriella Xibilia. Soft sensor design for a topping process in the case of small datasets. *Computers & Chemical Engineering*, 35(11):2447–2456, 2011.
- [90] L Fortuna, S Graziani, G Napoli, and MG Xibilia. Stacking approaches for the design of a soft sensor for a sulfur recovery unit. In *IEEE Industrial Electronics, IECON 2006-32nd Annual Conference on*, pages 229–234. IEEE, 2006.
- [91] Hervé Abdi. Partial least square regression (pls regression). *Encyclopedia for research methods for the social sciences*, 6(4):792–795, 2003.
- [92] Herman Wold. Partial least squares. *Encyclopedia of statistical sciences*, 1985.
- [93] Carl Edward Rasmussen and Christopher KI Williams. Gaussian processes in machine learning. *Lecture notes in computer science*, 3176:63–71, 2004.

- [94] Carl Edward Rasmussen and Christopher KI Williams. *Gaussian processes for machine learning*, volume 1. MIT press Cambridge, 2006.
- [95] Mark Ebden. Gaussian processes: A quick introduction. *arXiv preprint arXiv:1505.02965*, 2015.